Bioactive Materials 17 (2022) 1–17

Contents lists available at ScienceDirect

Bioactive Materials

journal homepage: www.keaipublishing.com/en/journals/bioactive-materials

Glucose and MMP-9 dual-responsive hydrogel with temperature sensitive self-adaptive shape and controlled drug release accelerates diabetic wound healing

Wanyi Zhou [a,b,c], Zhiguang Duan [a,b,c], Jing Zhao [a,b,c], Rongzhan Fu [a,b,c,**], Chenhui Zhu [a,b,c,*], Daidi Fan [a,b,c,***]

[a] Shaanxi Key Laboratory of Degradable Biomedical Materials, School of Chemical Engineering, Northwest University, Xi'an, 710069, Shaanxi, China
[b] Shaanxi R&D Center of Biomaterials and Fermentation Engineering, School of Chemical Engineering, Northwest University, Xi'an, 710069, Shaanxi, China
[c] Biotech. & Biomed. Research Institute, Northwest University, Xi'an, 710069, Shaanxi, China

ARTICLE INFO

Keywords:
Dual-responsive
Temperature-sensitive
Shape self-adaptive hydrogels
Diabetic wound healing

ABSTRACT

Chronic diabetic wounds are an important healthcare challenge. High concentration glucose, high level of matrix metalloproteinase-9 (MMP-9), and long-term inflammation constitute the special wound environment of diabetic wounds. Tissue necrosis aggravates the formation of irregular wounds. All the above factors hinder the healing of chronic diabetic wounds. To solve these issues, a glucose and MMP-9 dual-response temperature-sensitive shape self-adaptive hydrogel (CBP/GMs@Cel&INS) was designed and constructed with polyvinyl alcohol (PVA) and chitosan grafted with phenylboric acid (CS-BA) by encapsulating insulin (INS) and gelatin microspheres containing celecoxib (GMs@Cel). Temperature-sensitive self-adaptive CBP/GMs@Cel&INS provides a new way to balance the fluid-like mobility (self-adapt to deep wounds quickly, approximately 37 °C) and solid-like elasticity (protect wounds against external forces, approximately 25 °C) of self-adaptive hydrogels, while simultaneously releasing insulin and celecoxib on-demand in the environment of high-level glucose and MMP-9. Moreover, CBP/GMs@Cel&INS exhibits remodeling and self-healing properties, enhanced adhesion strength (39.65 ± 6.58 kPa), down-regulates MMP-9, and promotes cell proliferation, migration, and glucose consumption. In diabetic full-thickness skin defect models, CBP/GMs@Cel&INS significantly alleviates inflammation and regulates the local high-level glucose and MMP-9 in the wounds, and promotes wound healing effectively through the synergistic effect of temperature-sensitive shape-adaptive character and the dual-responsive system.

1. Introduction

Chronic diabetic wounds are a serious complication of diabetes, which often leads to high costs of treatment and high rates of amputation [1,2]. Many studies have attempted to explore the causes of chronic diabetic wound non-healing due to the difference in the physiological environment of acute and chronic wounds [3]. The healing of normal wounds includes haemostasis, inflammation, proliferation, and remodelling; however, high concentrations of glucose and matrix metalloproteinases (MMPs) in the wound microenvironment cause hindrance for chronic diabetic wounds to enter the tissue remodelling phase [4–8]. Prolonged hyperglycaemia leads to advanced glycation end-products

; MMP-9, matrix metalloproteinase-9; PVA, polyvinyl alcohol; INS, insulin; GMs, gelatin microspheres; Cel, celecoxib; MMPs, matrix metalloproteinases; AGEs, advanced glycation end-products; CBP, the CS-BA-PVA hydrogel; VEGF, vascularendothelialgrowthfactor; CS, chitosan; STZ, streptozotocin; BA, Carboxyphenylboric acid; TNF-α, Tumornecrosisfactor-α; IL-10, interleukin-10.

Peer review under responsibility of KeAi Communications Co., Ltd.

* Corresponding author. Shaanxi Key Laboratory of Degradable Biomedical Materials, School of Chemical Engineering, Northwest University, Xi'an, 710069, Shaanxi, China.

** Corresponding author. Shaanxi Key Laboratory of Degradable Biomedical Materials, School of Chemical Engineering, Northwest University, Xi'an, 710069, Shaanxi, China.

*** Corresponding author. Shaanxi Key Laboratory of Degradable Biomedical Materials, School of Chemical Engineering, Northwest University, Xi'an, 710069, Shaanxi, China.

E-mail addresses: 20175112@nwu.edu.cn (R. Fu), zch2005@nwu.edu.cn (C. Zhu), faidaidi@nwu.edu.cn (D. Fan).

https://doi.org/10.1016/j.bioactmat.2022.01.004
Received 9 October 2021; Received in revised form 15 December 2021; Accepted 4 January 2022
Available online 19 January 2022

(AGEs) accumulation in skin tissues, resulting in a series of changes in histology and cytology, such as cell dysfunction and reduced secretion of multiple growth factors, especially inflammatory cell dysfunction, which exacerbates and prolongs the inflammatory phase of chronic diabetic wounds [9–11]. Aberrant inflammation causes the upregulated secretion of pro-inflammatory factors, further disturbing the balance of MMPs and tissue inhibitors of metalloproteinases (TIMPs) and leads to the oversecretion of MMPs in wounds, especially the amount of MMP-9—which was enhanced 14 times in diabetic ulcers than in traumatic wounds [4,12–14]. The high concentration of MMPs, which degrade a variety of growth factors and matrix proteins required for wound healing, is considered as one of the main reasons for the transformation of acute wounds into chronic wounds [3,4]. Consequently, MMP-9 is regarded as a novel target for the treatment of chronic diabetic wounds [15]. In addition, another factor that affects the healing of diabetic wounds is the irregular shape of wounds after removing the necrotic tissues; traditional clinical dressings give rise to a higher risk of infection due to their quite unfitting shape of the irregular wounds [16–19]. Overall, it is necessary to develop a wound dressing that fully adapts to the wound shape as well as regulates the level of MMP-9 and glucose, thereby accelerating the healing of chronic diabetic wounds.

Hydrogels are reasonable wound dressings that create a moist environment for wounds, absorb tissue exudates, and transport functional drugs to accelerate wound healing. In recent years, stimuli-responsive drug-loaded hydrogels have attracted much attention in biomedicine, as they respond to the external environment—such as reactive oxygen species (ROS) [20,21], temperature [22], pH [23,24], glucose [23], enzymes [8,9]—and provide "smart" control for the release of drugs. High concentration of glucose and MMP-9 are important factors hindering chronic diabetic wound healing [6,14], and the double-stimulus responsive drug-loaded hydrogel targeting glucose and MMP-9 is a promising dressing. Moreover, most drug-loaded hydrogels are hard to change their shape again after molding, indicating that they are not fully self-adaptive to ever-varying inner wound tissues, especially chronic diabetic foot wounds that are constantly deformed during movement [19]. Self-adaptive hydrogels, constructed based on the phenomenon of fluid quickly filling irregular containers, are a solution to the above issues [25]. However, the fluid-like and solid-like properties of traditional self-adaptive hydrogels, which consist of dynamic covalent bonds (such as borate bonds [19,26], Schiff base reactions [25,27]) or non-covalent bonds (such as hydrogen bonds) are difficult to balance. Self-adaptive hydrogels with more fluid-like properties are difficult to provide with enough mechanical properties (the cohesive force) to resist forces and protect the wounds; hydrogels with more solid-like properties cannot easily fill irregular deep wounds quickly. Thus, a novel hydrogel dressing for treating chronic diabetic wounds is eagerly awaited, which should meet the needs of chronic diabetic wounds with high levels of glucose and MMP-9 and long-term inflammation, fully adaptable to the irregular shaped wounds while providing sufficient protection for the wounds.

In this study, we designed a glucose and MMP-9 dual-responsive hydrogel with temperature-sensitive shape self-adaptive behaviors for the treatment of chronic diabetic wounds (Scheme 1). To our knowledge, this is the first attempt to construct a glucose and MMP-9 dual-responsive hydrogel with temperature sensitive self-adaptive shape. When the hydrogel was exposed to chronic diabetic wounds, temperature-sensitive self-adaptability ensured that the hydrogel on-demand provided mobility and elasticity to quickly adapt and protect wounds, at the same time, the glucose and MMP-9 double-response system facilitated the on-demand release of insulin (INS) and anti-inflammatory drug (celecoxib (Cel)). For the temperature-sensitive self-adaptability of hydrogels, we drew on the temperature-dependent viscoelasticity of polymers formed by borate ester bonds [26,28]. The hydrogel was more liquid-like at the body temperature (approximately 37 °C) and more solid-like at room temperature (approximately 25 °C); therefore, the hydrogel filled the deep wounds owing to the fluid-like properties and protected the wounds by the solid-like properties at the skin wound temperature, and the hydrogel was more shape self-adaptive for deeper wounds. For the glucose and MMP-9 dual-responsive system, we uniformly dispersed celecoxib-loaded gelatin microspheres (GMs@Cel) and insulin (INS) in the CS-BA-PVA hydrogel (CBP) which was constructed using phenylboronic acid-modified chitosan (CS-BA)

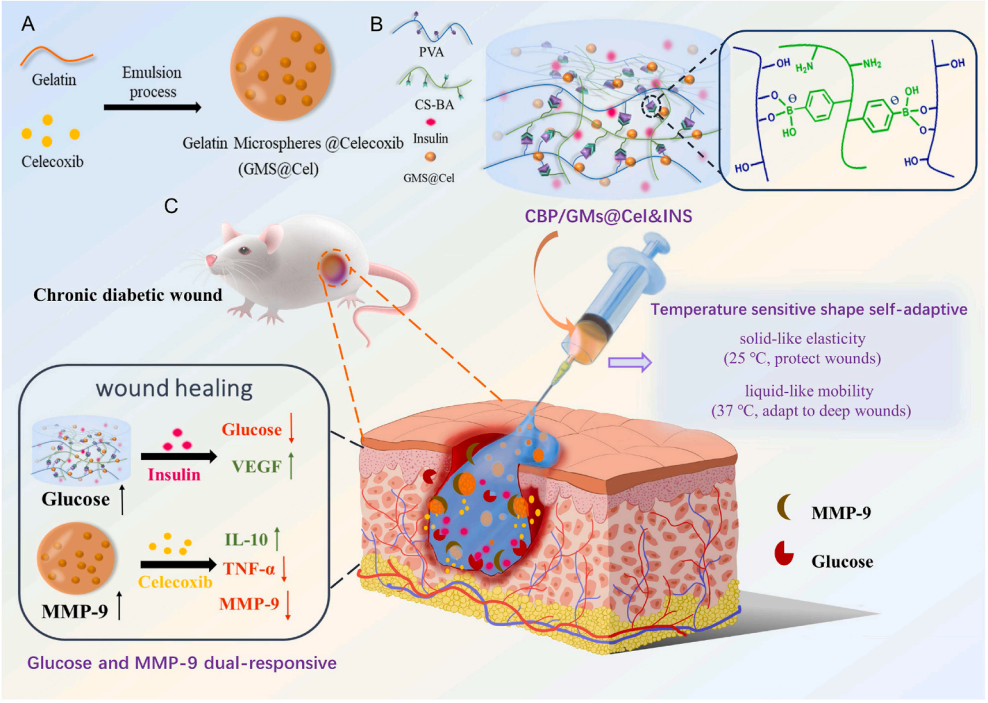

Scheme 1. The design strategy of glucose and MMP-9 dual-responsive shape self-adaptive hydrogels for treating chronic diabetic wound. (A) Preparation of gelatin microspheres containing celecoxib (GMs@Cel). (B) Preparation of the CBP/GMs@Cel&INS hydrogel and the characteristics of temperature sensitive shape self-adaptive. (C) The process of treating chronic diabetic wounds with the CBP/GMs@Cel&INS hydrogel through the glucose and MMP-9 dual-response system.

and polyvinyl alcohol (PVA) via phenylborate ester bonds. The CBP network was hydrolysed to release insulin (INS) and GMs@Cel through glucose-induced phenylborate ester bond breaking, and the abundant amino groups on chitosan reduced the pKa of the phenylborate ester bond to enhance the sensitivity of the hydrogel to glucose at pH 7.4 [29]. Celecoxib in GMs@Cel was released through the degradation of gelatin (an inherent degradation substrate of MMP-9) under the action of MMP-9. Moreover, the double encapsulation of microspheres and the hydrogel prevented the sudden release of small molecule celecoxib, the monolayer encapsulation of the hydrogel ensured the sensitive release of macromolecule insulin, thus promoting the full uptake of insulin and celecoxib by cells. In short, the CBP/GMs@Cel&INS hydrogel accelerated the healing of chronic diabetic wounds by (i) full adapting to irregular wounds, (ii) anti-inflammatory effects, (iii) regulating the local levels of glucose and MMP-9 in the wounds, (iv) promoting the secretion of vascular endothelial growth factor (VEGF).

2. Experimental section

2.1. Materials

PVA (99.0% alcoholysis, Mr ~ 89,000–98,000), gelatin (>98%), chitosan (CS) (MW~100000 Da) was supplied by Shanghai Macklin Biochemical Co., Ltd. (China). Bovine insulin, celecoxib, and streptozotocin (STZ) were obtained from Sigma-Aldrich (USA). 3-Carboxyphenylboric acid (BA), N-hydroxysuccinimide (NHS), 1-(3-Dimethylaminopropyl)-3-ethylcarbodi-imide hydrochloride (EDC.HCl), and all other chemicals were purchased from Shanghai Aladdin Bio-Chem Technology Co., Ltd. (China). 5-Ethynyl-2′-deoxyuridine (EdU) and all enzyme linked immunosorbent assay (ELISA) kits were from Multisciences (Lianke) Biotech, Co., Ltd. (China). Tumor necrosis factor-α (TNF-α) antibody, interleukin-10 (IL-10) antibody, vascular endothelial growth factor (VEGF) antibody and matrix metalloproteinase-9 (MMP-9) antibody were provided by Servicebio Biotech, Co., Ltd. (China); and advanced glycation end products (AEGs) antibody was from Bioss Biotech, Co., Ltd. (China).

2.2. Synthesis of 3-carboxylicphenylboric acid modified chitosan (CS-BA)

In accordance with previous studies [23], 2 g of CS was dissolved in 800 mL of 0.3% acetic acid, according to the unit molar ratio of CS: BA: EDC: NHS = 1: 2: 2.5: 2.5, 3-carboxyphenyl boric acid, EDC, and NHS dissolved in 40 mL methanol (pH = 5.0) and added to the CS solution. The mixture was stirred for 24 h. The mixture was dialysed with ultrapure water for 3 days, during which time the water was changed at least eight times.

2.3. Synthesis of gelatin microspheres (GMs) and gelatin celecoxib-loading microspheres (GMs@Cel)

According to previous reports [9], GMs were prepared using an emulsion process. In brief, Span 80 (0.5 mL) was added to 30 mL of paraffin liquid and stirred for 15 min at 1000 rpm at 45 °C for 30 min to form an oil phase. A 20 wt% gelatin aqueous solution was prepared, and the gelatin aqueous solution was slowly dropped into the oil phase at a volume ratio of gelatin solution (water phase): paraffin liquid (oil phase) = 6:1, stirring at 1000 rpm for 30 min. Then, the mixture was quickly transferred to an ice-water bath, where 1 mL of 15% glutaraldehyde solution was added and stirred for another 30 min. The mixture was alternately washed several times with diethyl ether and isopropyl alcohol, the organic solvent was removed using a rotary evaporator, and the GMs were eventually lyophilized. To prepare GMs@Cel, 8 mg celecoxib was added to 5 mL of 20% (wt%) gelatin aqueous solution and evenly mixed to form an aqueous phase; the remaining steps were the same as those used for preparing the GMs.

2.4. Preparation of CBP/GMs hydrogels (CBP/GMs@Cel&INS hydrogels)

A 5% (wt%) CS-BA solution and 16.7% (wt%) PVA solution were prepared with deionised water, 0.4 mL CS-BA solution, 0.6 mL PVA solution, and 0.15 g GMs were mixed evenly. To prepare CBP/GMs@Cel&INS hydrogel, according to the method of preparing CBP/GMs, mixing CS-BA and PVA solution, adding 1.28 mg/mL insulin (INS) and 0.15 g GMs@Cel in the mixture of CS-BA and PVA solution.

2.5. Characterisation

The structure of CS-BA was confirmed by ^{1}H nuclear magnetic resonance (^{1}H NMR, Bruker 400M, Germany) and Fourier-transform infrared spectroscopy (FT-IR, Thermo Fisher Scientific, Waltham, MA, USA). The size distribution of the microspheres was measured using a laser particle size analyser (Mastersizer 3000, Malvern, UK). The structures of the microspheres and hydrogels were observed using a scanning electron microscope (SEM; Carl Zeiss, Oberkochen, Germany).

2.6. Drug loading and release

The CBP/GMs@Cel&INS hydrogels (1 g) were placed in 5 mL of media (phosphate-buffered saline containing different concentrations of glucose and MMP-9, 2% (v/v) Tween 80) at 37 °C. At the required time point, the release solution (0.5 mL) was collected from the media, and fresh media (0.5 mL) was added after each sampling to maintain a constant volume of the total medium. The insulin released was measured using enzyme linked immunosorbent assay (ELISA) kits (Multisciences, China), and the celecoxib released was determined by reversed-phase high-performance liquid chromatography (RP-HPLC) with a UV detector set at 254 nm. The sample (20 μl) was injected into a Diamonsil C18 column (250 mm × 4.6 mm, 5.0 μm, Dikma, USA) and eluted with a mobile phase consisting of ultrapure water/methanol (15/85, v/v) at a flow rate of 1 mL/min. On average, three repeated tests were used to plot the release results.

2.7. Rheological tests

The rheological properties of the hydrogels were determined using a rheometer (Anton Paar, MCR302). Rheological testing of hydrogels includes (1) time sweep tests of hydrogels (25 °C), a constant frequency of 25 rad/s, and a constant strain of 0.05%. (2) Frequency scanning of the hydrogels. The scanning frequency varied from 0.1 to 100 rad/s, and the constant strain of the frequency scanning test was 0.05%. (3) Strain amplitude sweep tests of the hydrogels (25 °C), the constant frequency of 25 rad/s (4) The G′ and G″ of hydrogels (25 °C) from alternate-step strain sweep, the constant frequency of 25 rad/s, when the alternate step strain was switched from a small strain of 0.05% and a large strain of 200%.

2.8. Adhesion strength test of hydrogels

The adhesive properties of the hydrogels were determined using a lap shear test at 25℃. Briefly, two pieces of porcine skin tissue were cut into rectangles of 10 mm × 80 mm, and grease was thoroughly removed from the porcine skin tissues before use. Hydrogels (0.02 g) were used to adhere to two pieces of porcine skin tissue, and the adhesive area was 10 mm × 10 mm. The samples were tested on a tensile testing machine (INSTRON 5565, Instron, Norwood, MA, USA) at a speed of 10 mm/min until two pieces of skin tissue were separated. The adhesive strength was calculated based on the maximum modulus of the adhesive area.

2.9. Biocompatibility, cell proliferation and migration

The hydrogel extraction solution was used to evaluate the

biocompatibility of the hydrogels. After disinfection with radiation, hydrogels were immersed in the Roswell park memorial institute-1640 cell medium (RPMI-1640) for 72 h at 0.1 g/mL. The mouse fibroblasts (L929 cells) were incubated for 24 h. Then, the extraction solution of the hydrogels was added. One day and three days later, the absorbance of each well was measured to calculate the L929 cell viability, and acridine orange-ethidium bromide (AO-EB) staining kits were used with AO-EB stain the L929 cells. Each test was repeated six times. Glucose and MMP-9 damaged cells were used to evaluate the effect of the hydrogels on cell proliferation. In short, the L929 cells were cultured in RPMI-1640 cell medium containing 10 mg/ml glucose, 50 nM MMP-9, and 0.1 g/mL hydrogel for one day and three days. Cell viability was then calculated, and each test was performed in sextuplicate. The effect of hydrogels on cell migration was evaluated using a cell scratch test. L929 cells were cultured for 24 h, and the cell layer was scratched with a 200 μL pipette tip; the cells were then treated with RPMI-1640 cell medium containing hydrogels, RPMI-1640 cell medium containing insulin (0.32 mg/mL), and RPMI-1640 cell medium containing 5 mg/mL glucose. Cells were incubated for 12 and 24 h, and wound closure was observed. Human umbilical vein endothelial (HUVEC) cells were cultured in different environments for 24 h, the concentration of glucose was 5 mg/mL, hydrogels were 0.1 g/mL, and drugs containing 0.32 mg/mL insulin and 0.3 mg/mL celecoxib. The proliferation activity of HUVECs was evaluated by a BeyoClick™ EdU Cell Proliferation Kit, and the results were observed by laser confocal microscopy.

2.10. Glucose consumption of L929 cells

L929 cells were cultured in RPMI-1640 cell medium for 24 h, and then cultured in RPMI-1640 cell medium containing 5 mg/mL glucose for 24 h (different concentrations of insulin and hydrogels loaded with corresponding concentrations of insulin were added respectively). Glucose consumption of L929 cells was measured using a glucose assay kit (Changchun Huili Biotech, Co., Ltd, China).

2.11. In vitro anti-inflammatory properties of hydrogels

RAW 264.7 macrophages were cultured in 6-well plates for 24 h in dulbecco's modified eagle medium (DMEM) containing 1 μg/mL LPS. Next, RAW 264.7 macrophages were incubated with serum-free DMEM containing 1 μg/mL LPS and 0.1 g/mL hydrogel for another 24 h in each well. Finally, TNF-α, IL-10, and MMP-9 were detected using ELISA kits and immunofluorescent staining.

2.12. Diabetic rat model of full skin defect

The animal experiments of this study followed the guidelines set of experimental animal management and welfare ethics of Northwest University (China) (NWU-AWC-20210314R). Rats with type 1 diabetes were induced with STZ. Each rat was intraperitoneally injected with STZ at a dose of 65 mg/kg body weight. The SD rats were 8-weeks-old when they were first injected with STZ to induce diabetes, and hyperglycemia was confirmed when blood glucose levels were stable above 300 mg/dL. The full-thickness skin defect model was established after 24 days of stable blood glucose, and the blood glucose of SD rats was recorded until the complete wound healing. Diabetic rats (male, 14 weeks old) were randomly divided into five groups (n = 6). After the rats were anesthetized and shaved, two full skin defect wounds (8 mm in diameter) were formed on the back of each rat. After rinsing with normal saline, the rats were treated in different ways: (1) dressing the wounds with gauze (the gauze group, the control group), (2) treating the wounds with commercial dressing (the HeraDerm group, the commercial hydrogel control group); (3) 0.4 mL the CBP/GMs hydrogel (the hydrogel II group) was used to treat the wounds; (4) 0.4 mL the CBP/GMs@INS hydrogel (the hydrogel III group) to cover the wounds; (5) treating the wounds with 0.4 mL the CBP/GMs@Cel&INS hydrogel (the hydrogel Ⅳ group). The hydrogels were injected through a syringe to cover wounds with full skin defects. And hydrogels were changed every 48 h in the healing process. A camera was used to record the wound area, and blood glucose levels were continuously monitored during the experiment.

2.13. Histological analysis

The wound sections of rats were stained with hematoxylin and eosin (H&E), AGEs, MMP-9, TNF-α, IL-10, and VEGF antibodies to analyse the wound healing mechanism under standard procedures.

2.14. Statistical analyses

SPSS (IBM SPSS statistical 19) software was used for statistical analysis, and the results were expressed as the mean ± standard deviation (SD), and the results of significant differences were as follows: *P $<$ 0.05, **P $<$ 0.01, ***P $<$ 0.001).

3. Results and discussions

3.1. Synthesis and characterisation of the hydrogels

To promote the healing of chronic diabetic wounds, medical polymer PVA and good biocompatibility of natural polymers such as CS and gelatin were used as the main materials of the hydrogels. Gelatin microspheres containing celecoxib (GMs@Cel) were prepared by an emulsion process, and the network of the hydrogel was cross-linked by 3- carboxyphenylboric acid-modified chitosan (CS-BA) and PVA through phenylborate ester bonds. The synthesis route of CS-BA is shown in Figs. 1A and S1A. After the carboxyl group of 3-Carboxyphenylboronic acid was activated by EDC.HCl and NHS, the boric acid group was introduced into the polymer chain of CS through a coupling reaction between the amino group in chitosan and the carboxyl group in 3-Carboxyphenylboronic acid. To confirm the successful modification of chitosan, CS-BA was characterised by FT-IR and ^{1}H NMR spectroscopy. As shown in FT-IR (Fig. 1B), C–H out-of-plane bending bands of aromatics appeared at 770 cm^{-1}, while characteristic absorption band of benzene ring appeared at 1550 cm^{-1}, and in the ^{1}H NMR spectrum (Fig. 1C), the characteristic peaks of the phenyl group protons at 7.4, 7.8 and 8.2 PPM, the peak at 2.9 PPM was assigned to methylene protons of succinic acid on CS backbone, and a peak appeared at 3.66 PPM was considered to be the protons of C2–C6 on CS units, this fully proved that the modification of chitosan by 3-Carboxyphenylboronic acid was successful. Furthermore, the peak of the B–O formed by the boric acid part of CS-BA and the cis dihydroxyl group of PVA was sharp at 1340 cm^{-1}, indicating the formation of the CBP hydrogel and the CBP/GMs (Fig. S1C and Fig. S1D). Imine group (-C═N-) appeared at 1643 cm^{-1}, which indicated the successful synthesis of gelatin microspheres (GMs) cross-linked by Schiff's base reaction (Fig. S1C), and the amide group (N–H) appeared at 1548 cm^{-1} was attributed to the fact that the microspheres are composed of gelatin (Fig. S1D). To obtain the optimal CBP/GMs@Cel&INS hydrogel, the gelation time of the CBP hydrogel was further optimised, and the final gelation time of the CBP hydrogel was controlled at 189 s (Fig. 1D). The structures of the selected CBP hydrogel were observed by SEM (Fig. 1E), which showed uniform porous structures with a pore size of approximately 5–30 μm, and the porosity of the CBP hydrogel and the CBP@GMs hydrogel were respectively 50.44 ± 3.53% and 29.98 ± 2.36% (Fig. S1B). The encapsulation efficiency (EE %) and drug loading efficiency (DL%) of GMs@Cel were 84.03 ± 5.78% and 9.6 ± 1.18%, respectively (Figs. 1F and S1E); GMs@Cel were smooth microspheres with a diameter of approximately 50–100 μm (Fig. 1G). In addition, Fig. 1H shows the formation of the CBP/GMs@Cel&INS hydrogel by mixing the mixed solution of CS-BA and insulin (INS) (CS-BA@INS), PVA solution, and gelatin celecoxib-loading microspheres (GMs@Cel).

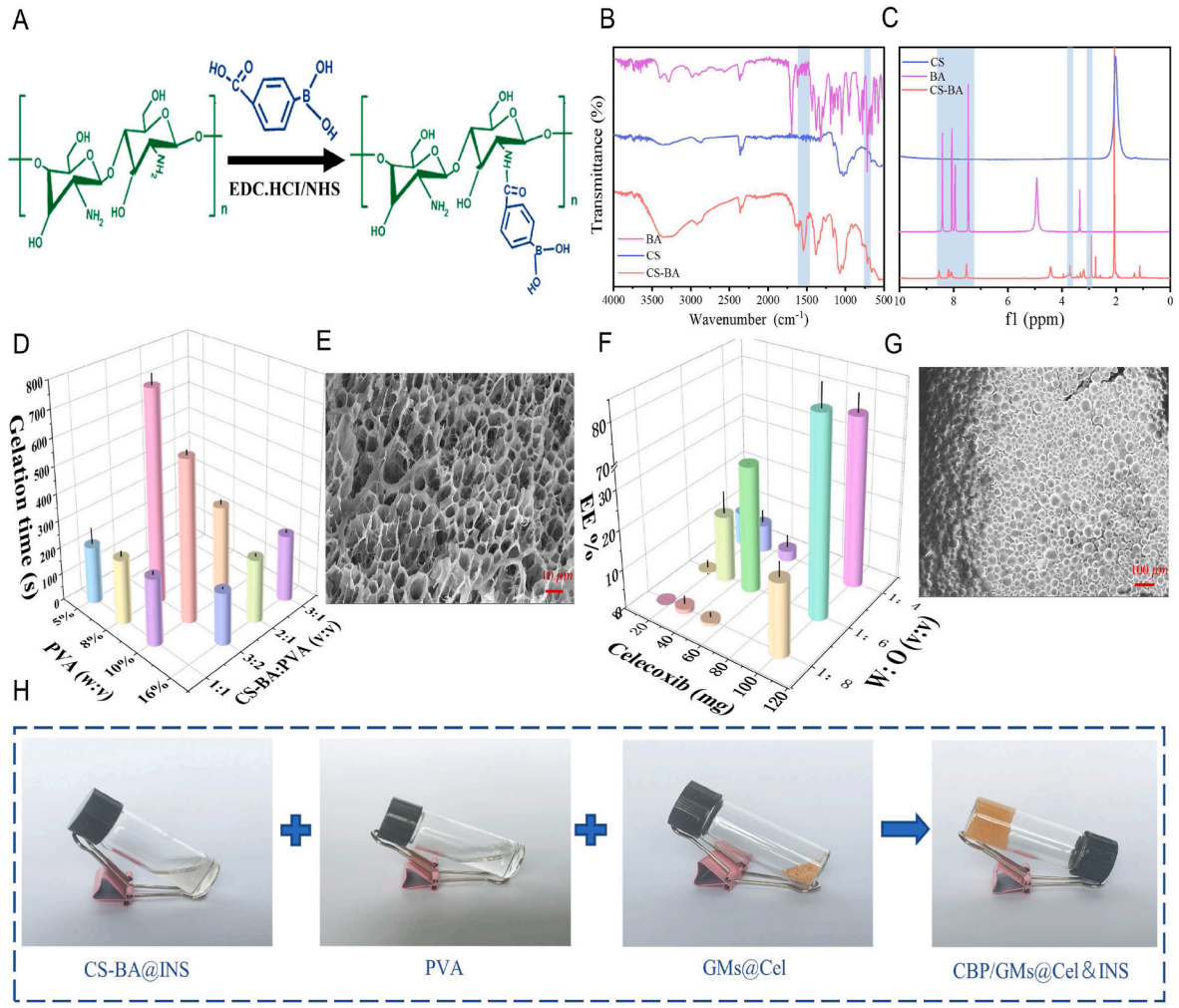

Fig. 1. Characterisation of polymers and hydrogels. (A) A synthetic scheme of CS-BA polymer. (B) FT-IR spectra of CS, BA, CS-BA. (C) ^{1}H NMR spectra of CS, BA, CS-BA. (D) Optimisation of gelation time of CBP hydrogel (tested by the vial inverting method). (E) The porous structure of the CBP hydrogel, characterised by SEM on a scale of 10 μ m. (F) Optimisation of encapsulation efficiency (EE%) of GMs@Cel (X axis: weight of celecoxib fed initially (mg); Y axis: water phase: oil phase (V: V)). (G) the SEM characterisation of GMs@Cel, scale bar was 100 μ m. (H) photographs of CS-BA@INS, PVA, and GMs@Cel assembled into a CBP/GMs@Cel&INS hydrogel.

3.2. Shape self-adaptive, remodelling, injectable, self-healing properties, and rheological curve analysis of hydrogels

Chronic diabetic wounds often develop into irregular wounds after repeated debridement, and frequently active and bent feet are the high-risk parts of chronic diabetic wounds. Traditional drug-loaded hydrogels cannot completely fill the constant deformation of irregular wounds in motion, resulting in a decrease in the drug release efficiency and an increase in the risk of wound infection; therefore, a temperature-sensitive shape self-adaptive CBP/GMs@Cel&INS hydrogel was designed. To simulate the irregular chronic diabetic wound, some beads with diameters of 6 mm were packed in beakers (Fig. 2A), CBP/GMs@Cel&INS cross-linked by phenylborate ester bonds flowed slowly under gravity to fill the gaps among the beads. at different temperatures, the speed of the CBP/GMs@Cel&INS hydrogel filled the gaps among the beads. At 45 °C, the hydrogel was more fluid-like; at 37 °C, the mobility of CBP/GMs@Cel&INS was weak, and at 25 °C, the CBP/GMs@Cel&INS hydrogel was more solid-like and less mobile. The temperature of skin wounds is between room temperature and body temperature, and the solid-like and liquid-like properties of CBP/GMs@Cel&INS reach a relative balance in this temperature range. Under the influence of ambient temperature and specific heat capacity of hydrogel, the part of hydrogel staying on the skin surface was close to room temperature and had more solid-like elasticity to protect the wound. while the other part of the hydrogel in the deep wound was close to body temperature and was more fluid-like mobility to self-adapt to ever-varying inner wound tissues. In addition, the CBP/GMs@Cel&INS hydrogel could be injected into the wound through a 1.6 × 30 mm needle and a 0.7 × 32 mm needle at 45 °C (Fig. 2B). The above results show that the temperature-sensitive shape self-adaptive properties of the CBP/GMs@Cel&INS hydrogel provided convenience for clinical application and more intelligent wound protection.

In contrast to some hydrogels which are usually formed by rigid covalent networks, the CBP/GMs@Cel&INS hydrogel has the properties of remodelling and self-healing owing to the formation-breaking cycle of phenylborate ester bonds [30]. The spherical hydrogel could be remoulded to the maple leaf hydrogel (Fig. 2C), Fig. 2D, S2A and supplementary video showed the rapid self-healing of CBP/GMs@Cel&INS and the recovery of mechanical properties after self-healing at 25 °C. The self-healing and remodeling properties of fractured CBP/GMs@Cel&INS prolonged its service life as a wound dressing.

Supplementary video related to this article can be found at https://doi.org/10.1016/j.bioactmat.2022.01.004

To further understand the temperature-sensitive self-adaptability of the CBP/GMs@Cel&INS hydrogel, we performed rheological tests. As shown in Fig. 2F, dynamic frequency sweep measurements were carried

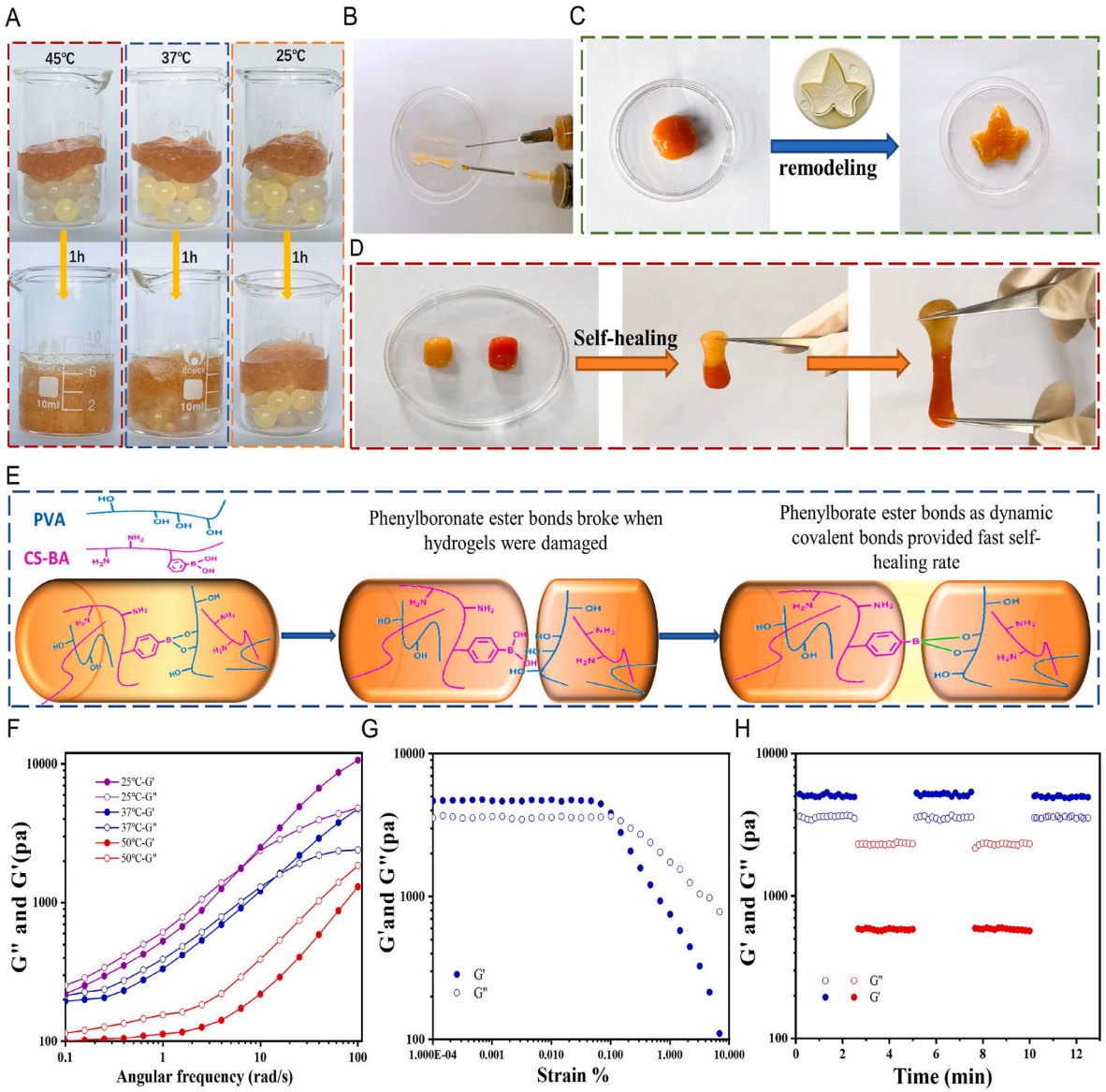

Fig. 2. Temperature-sensitive shape self-adaptive, self-healing, remodelling, injectable and rheological properties of the CBP/GMs@Cel&INS hydrogel. (A) Shape self-adaptive properties of the hydrogel at different temperatures. (B) Injectable properties of CBP/GMs@Cel&INS. (C) Remodelling properties of CBP/GMs@Cel&INS. (D) Self-healing properties of the hydrogel. (E) Self-healing mechanism of CBP/GMs@Cel&INS. (F) Frequency scanning test of CBP/GMs@Cel&INS. (G) Strain amplitude sweep of CBP/GMs@Cel&INS. (H) The G′ and G″ of CBP/GMs@Cel&INS from alternate-step strain sweep.

out at different temperatures, and the energy storage modulus (G′) and loss modulus (G″) of CBP/GMs@Cel&INS at 25 °C surpassed those obtained at 45 °C and 37 °C. The results showed that the fluidity of CBP/GMs@Cel&INS gradually increased as the temperature increased from 25 °C to 45 °C, which was consistent with the macroscopic experimental results in Fig. 2A. The increase in the G′ and G″ values of the CBP/GMs@Cel&INS hydrogel depended heavily on the increasing frequency, which is considered to be a notable feature of shape self-adaptive hydrogels [27], indicating that CBP/GMs@Cel&INS had liquid-like and solid-like properties at the same time; when CBP/GMs@Cel&INS was applied to the wound, it self-adapted to the wound with the fluid-like property (0.1–6 rad/s) and protected the wound with solid-like elasticity when confronted with external forces (15–100 rad/s), and CBP/GMs@Cel&INS was still a shape-adaptive hydrogel at 25 °C, although it had more solid-like characteristics. Moreover, the hydrogel at different temperatures always had the fluid-like properties at low angular frequencies (0.1–6 rad/s), this showed CBP/GMs@Cel&INS could adapt to various shapes at different temperatures, such as syringe needles, but the hydrogels needed to be quickly extruded from the syringe needle to ensure the convenience of clinical application, thus, we recommend CBP/GMs@Cel&INS be injected at slightly higher temperatures (approximately 45 °C). Fig. 2G shows the solid-like elasticity of the hydrogel (frequency 25 rad/s, 25 °C), and the hydrogel network collapsed at a strain of 0.15%. Although the hydrogel withstood a low strain, the hydrogel compensated for this deficiency by rapid self-healing after collapse. Strain amplitude sweep tests the stability of hydrogels under alternately transformed strains at 25 °C (Fig. 2H). The CBP/GMs@Cel&INS hydrogel was destroyed at 200% of strain, when the applied strain returned to 0.05%, the hydrogel rapidly returned close to the initial gel-like state, indicating that CBP/GMs@Cel&INS has good self-healing property, which is consistent with the macroscopic experimental results of Fig. 2D.

3.3. Double response of hydrogel and drug release in vitro

Considering the wound characteristics of chronic diabetic wounds,

we designed a glucose and MMP-9 dual-response hydrogel. The critical point of the sol-gel transformation was demonstrated by a time sweep rheological test (Fig. 3A). When the energy storage modulus (G′) was larger than the loss modulus (G″), the hydrogel changed from the fluid state to the gel state, and the gelation time of the hydrogel was within 3 s. However, when 5 mg/mL glucose was added to the medium, the G′ and G″ decreased obviously, indicating that high levels of glucose decreased the crosslinking density of the CBP/GMs@Cel&INS hydrogel network. This might be because phenylborate ester bonds were formed between phenylborate group and the hydroxyl group of glucose more easily than the hydroxyl group of PVA [31]. Thus, high glucose levels might promote the release of insulin and GMs@Cel by decomposing hydrogels. Moreover, gelatin as the definite substrate of MMP-9 [9], the size of the GMs@Cel became smaller and the shape of the GMs@Cel became irregular after 50 nM MMP-9 treatment for 72 h (Fig. 3B and C), this indicated that high concentration of MMP-9 could accelerate the release of celecoxib by degrading gelatin microspheres. The concentration of glucose in diabetic rats was about 5 mg/mL (Fig. S5B). And as shown in Fig. 3D, when the concentration of glucose increased from 0 to 5 mg/mL, the release of insulin increased from 36 ±2.23% to 75 ± 2.22% within 72 h. Fig. 3E and Fig. S4A showed that more celecoxib was released from the hydrogel at the higher concentration of MMP-9, when MMP-9 was changed from 0 nM to 50 nM, the release of celecoxib increased from 18 ±2.57% to 40 ±3.12% within 120 h. These results fully indicated that the CBP/GMs@Cel&INS hydrogel released insulin and celecoxib on demand in response to high levels of glucose and MMP-9. Importantly, the release of celecoxib reached 62.31 ±1.91% within 120 h under 5 mg/mL glucose and 50 nM MMP-9, suggesting that the disintegration of hydrogels could be accelerated by the synergistic effect of glucose and MMP-9. Fig. 3F showed that the CBP/GMs@Cel&INS hydrogel network was hydrolysed after treatment with 5 mg/mL glucose and 50 nM MMP-9 for 100 h. In addition, the release kinetics of insulin and celecoxib in different environments are shown in Figs. 3G and S3. Insulin was released following first-order kinetics, which was attributed to drug diffusion and hydrogel network swelling, suggesting that glucose reduced the crosslinking density of the

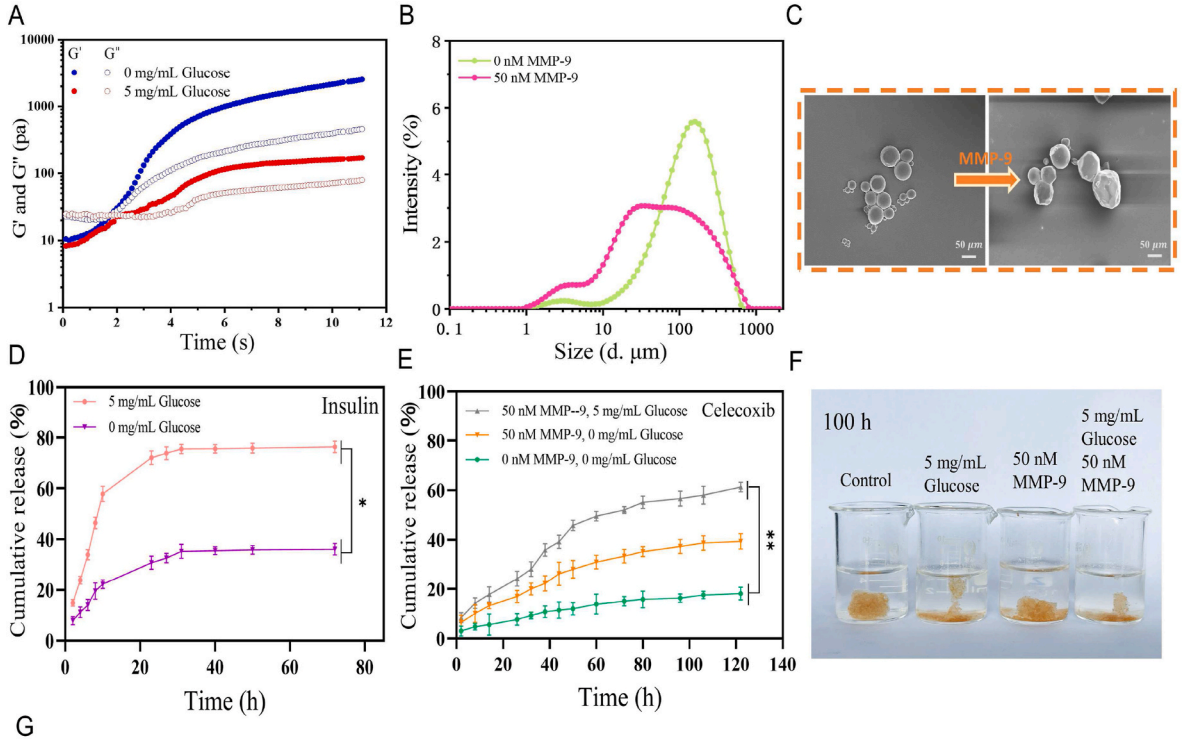

G

Release Kinetics				
Formulation Code	Zero Order	First Order	Korsmeyer Peppas	
	R^2	R^2	R^2	n
INS (0 mg/mL Glucose)	-0.20	0.99	0.89	0.36
INS (5 mg/mL Glucose)	-0.54	0.99	0.82	0.32
Cel (0 nM MMP-9)	0.62	0.98	0.98	0.50
Cel (50 nM MMP-9)	0.62	0.97	0.98	0.50
Cel (50 nM MMP-9, 5 mg/mL Glucose)	0.67	0.97	0.96	0.53

Fig. 3. In vitro release of the CBP/GMs@Cel&INS hydrogel via the glucose and MMP-9 dual response system. (A) G′ and G″ of the CBP/GMs@Cel&INS hydrogel on time sweep tests. (B) The size distribution of GMs@Cel treated with 50 nM MMP-9 for 72 h. (C) The changes of GMs@Cel after 50 nM MMP-9 treatment for 72 h. (D) The insulin cumulative release of the CBP/GMs@Cel&INS hydrogels. (E) The celecoxib cumulative release of the CBP/GMs@Cel&INS hydrogels. (F) a photograph that CBP/GMs@Cel&INS hydrogels were treated for 100 h under different concentrations of glucose and MMP-9. (G) The release kinetics of insulin and celecoxib.

CBP network and caused swelling of the hydrogel to release insulin. The release of celecoxib at 0 nM MMP-9 followed first-order kinetics, and that at 50 nM MMP-9 followed Korsmeyer-Peppas formula (n = 0.5), which might be due to the accelerated diffusion of celecoxib caused by the dissolution of gelatin at 50 nM MMP-9. In Korsmever Peppas kinetics, the release of celecoxib at 5 mg/mL glucose and 50 nM MMP-9 was consistent with non-Fickian diffusion caused by drug diffusion and polymer dissolution (n > 0.5), indicating that the swelling and collapse of CBP/GMs@Cel&INS hydrogels accelerated the release of celecoxib under the synergistic effect of glucose and MMP-9. In addition, the release of celecoxib at 5 mg/mL glucose and 50 nM MMP-9 environment was more consistent with first-order release kinetics, which might be due to the fact that celecoxib was released through both CBP hydrogel and GMs, indicating that the double-layer encapsulation of CBP hydrogel and gelatin microspheres was more effective in preventing the sudden release of the small molecule celecoxib.

3.4. Adhesive property of the hydrogels

Traditional hydrogel dressings should be fixed on gauze or other extra fixation methods, which causes the traditional hydrogel dressing to easily fall off and wound infection. Diabetic foot ulcers occur in the foot of regular exercise; thus, strongly adhering hydrogel dressings are required to follow the movement of diabetic wounds. Moreover, most of the hydrogels with tissue adhesion properties are focused on enhancing the interfacial force with the tissue to improve the adhesion properties of hydrogels, such as the mussels-inspired hydrogels [32], or oxidized dextran hydrogel via Schiff's base reaction with amines in tissue [33]. However, the effect of the physical properties of hydrogels on the enhancement of adhesive strength is often overlooked [34]. We believe that the frequency-dependent viscoelasticity of the CBP/GMs@Cel&INS hydrogel has a profound effect on its adhesion [27,34]. Fig. 4B was plotted as the damping factor tan (δ), the ratio of G″ to G′ represented the relative influence of viscous and elastic behaviour, this meant the viscosity of the hydrogels on long time scale (the CBP@INS hydrogel corresponded to 0.1–25 rad/s, and the CBP/GMs@Cel&INS hydrogel corresponded to 0.1–15 rad/s) and the elasticity of hydrogel on the short time scale (the CBP@INS hydrogel corresponded to 25–100 rad/s, and the CBP/GMs@Cel&INS hydrogel corresponded to 15–100 rad/s) existed simultaneously, therefore, on the one hand, due to the fluid-like properties of the CBP@INS and CBP/GMs@Cel&INS hydrogels at low frequencies, the two hydrogels completely fitted the uneven surface of the skin so that had sufficient adhesion areas with the skin for sufficient interfacial forces, on the other hand, the solid-like elasticity (cohesive force) of the two hydrogels at high frequencies allowed them to maintain elastic enough to withstand sudden forces. More importantly, the CBP/GMs@Cel&INS hydrogel changed from viscous dominance to elastic dominance faster than the CBP@INS hydrogel at low frequencies,

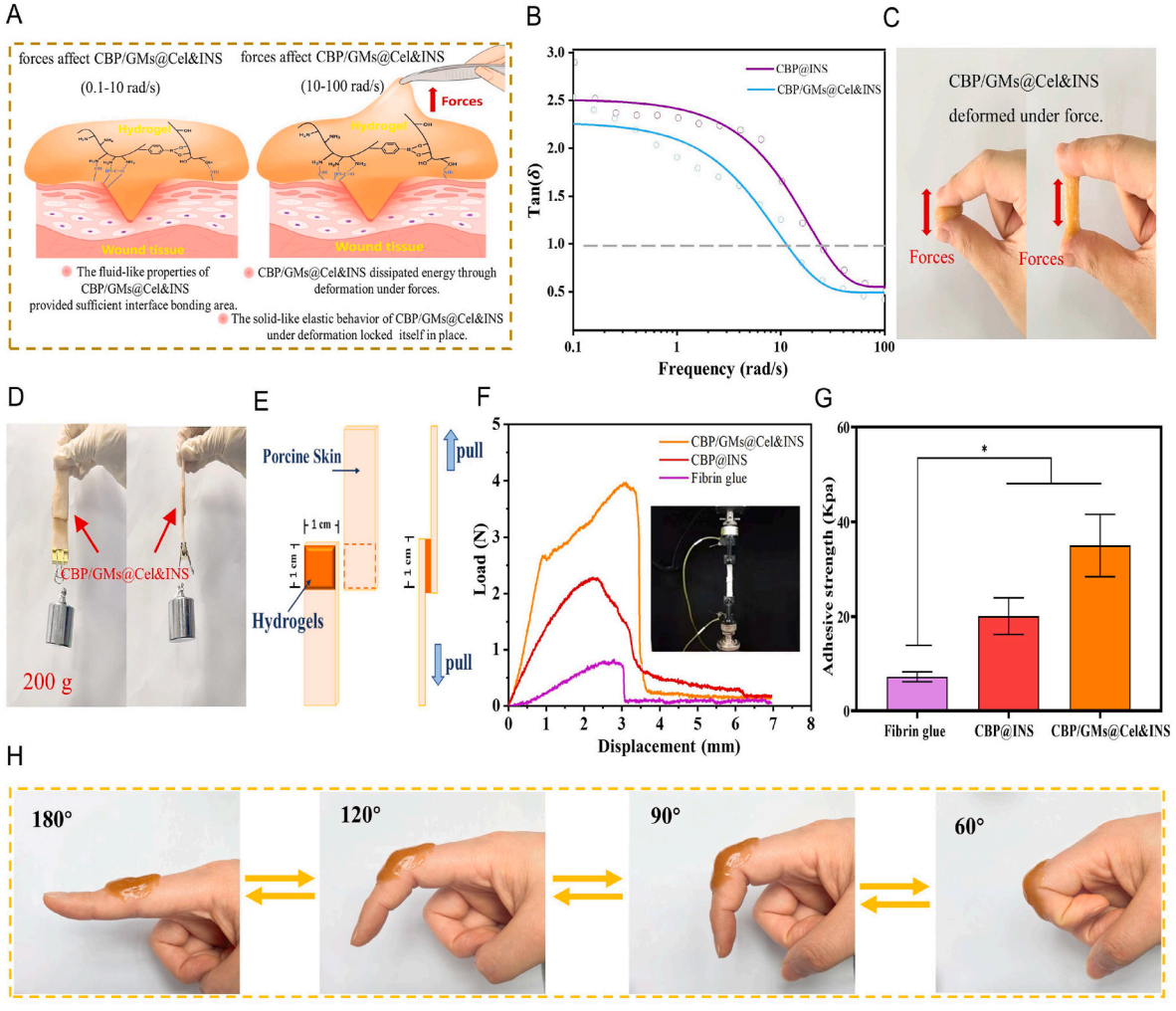

Fig. 4. Adhesion strength and adhesion mechanism of hydrogels. (A) The adhesion mechanism of the CBP/GMs@Cel&INS hydrogel. (B) Tan (δ) showed the frequency-dependent viscoelasticity required for hydrogels adhesion. (C) The deformation of the CBP/GMs@Cel&INS hydrogel under forces. (D) Adhesion properties of the CBP/GMs@Cel&INS hydrogel on porcine skin. (E) The mechanism of lap shear test for the adhesion of hydrogels to porcine skin. (F) Load-displacement curves of hydrogels on lap shear test of porcine skin. (G) Adhesion strength of hydrogels. (H) Adhesion of the CBP/GMs@Cel&INS hydrogel to moving joints.

indicating that the addition of GMs@Cel improved the rigidity and elasticity of the hydrogel; therefore, the CBP/GMs@Cel&INS hydrogel formed a durable bond with the skin without succumbing to weak destructive forces. In addition, as shown in Fig. 4C, when a CBP/GMs@Cel&INS hydrogel was stretched, it was deformed rather than stripped from the skin surface, indicating that the CBP/GMs@Cel&INS hydrogels as a dynamic network dissipated energy through deformation, resulting in a decrease in the forces acting on the adhesive interface, thus enhancing the adhesion strength of the hydrogel [35]. Fig. 4D showed two pieces of skin were tightly bonded together with a CBP/GMs@Cel&INS hydrogel (2.0 cm × 2.0 cm), and the hydrogel could maintain 200 g of weight, and the adhesive strength of hydrogels was evaluated employing a lap shear test at the room temperature [32] (Fig. 4F and G). The adhesive strength of the CBP@INS hydrogel was 22.83 ± 3.91 kPa, after adding gelatin microspheres, the adhesive strength of the CBP/GMs@Cel&INS hydrogel (39.36 ± 6.58 kPa) was five times larger than commercial fibrin glue (Bioseal®, (7.19 ± 1.04 kPa)). Moreover, the adhesive strength of the CBP/GMs@Cel&INS hydrogel exceeded that of many hydrogels with tissue adhesive properties [30,32,36]. The improvement in the adhesion of the CBP/GMs@Cel&INS hydrogel was due to the addition of micron-sized gelatin microspheres which enhanced the mechanical properties of the hydrogel (usually equal to the bonding force) [35,37], which is consistent with the results in Fig. 4B. Moreover, CS in the hydrogel also provided sufficient interface force through electrostatic and hydrophobic interactions with the skin [30].

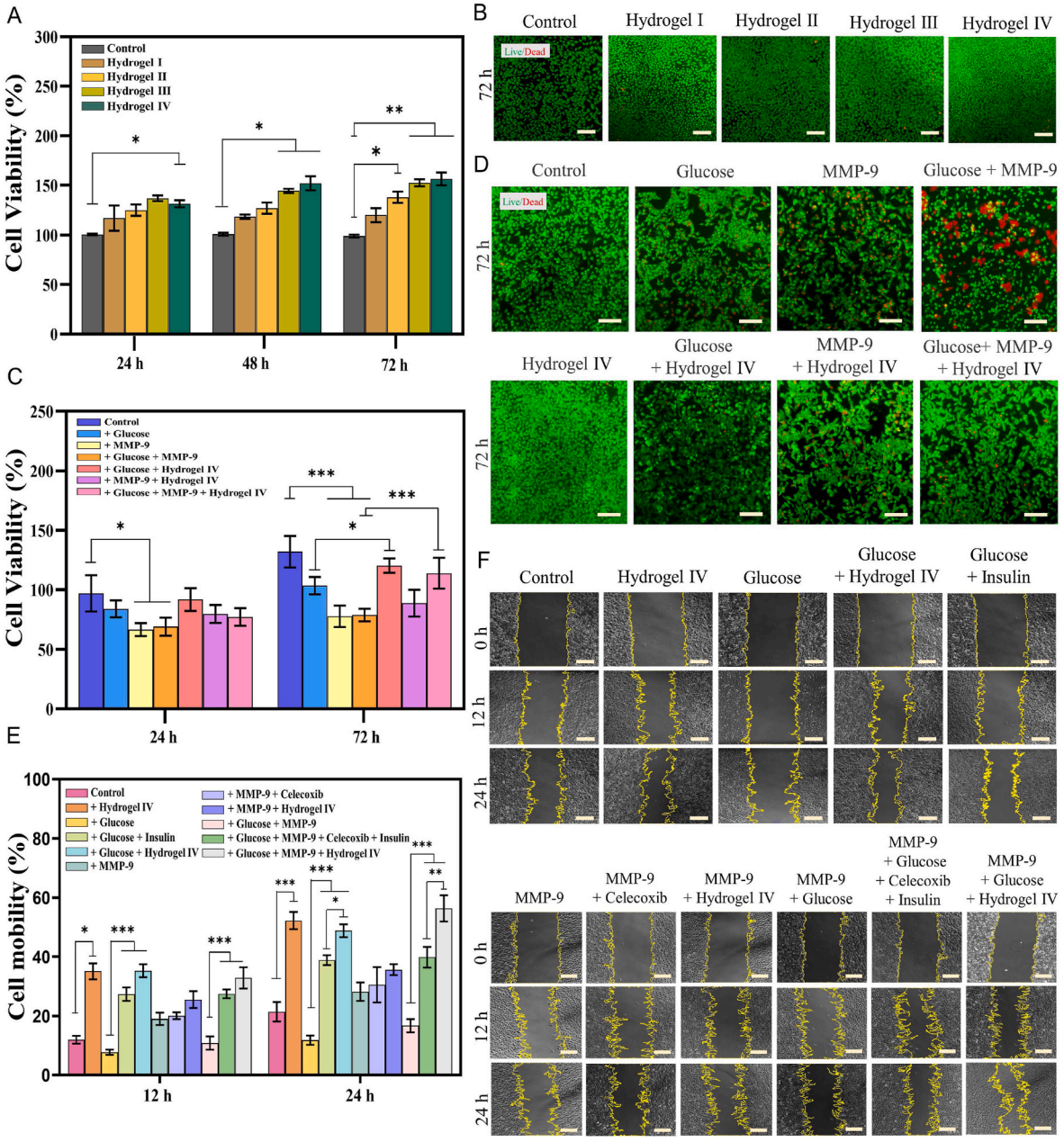

Fig. 5. The cytotoxicity, cell proliferation and cell migration ability of hydrogels. (A) Effects of different hydrogels on Cell viability of L929 cells for 24 h, 48 h and 72 h. (B) Live/dead staining of L929 cells cultured with different hydrogels for 72 h, scale bar: 100 *μm*. (C) Cell viability of L929 cells cultured in different environments for 24 h and 72 h. (D) Live/dead staining of L929 cells cultured in different environments for 72 h, scale bar: 100 *μm*. (E) Cell migration ability of L929 cells cultured in different environments for 12 h and 24 h. (F) Cell migration of L929 cells cultured in different environments for 12 h and 24 h, scale bar: 100 *μm*. Note: Hydrogel I: the CBP hydrogel; Hydrogel II: the CBP/GMs hydrogel; Hydrogel III: the CBP/GMs@INS hydrogel; Hydrogel Ⅳ: the CBP/GMs@Cel&INS hydrogel.

3.5. Promotion of cell proliferation and migration

Hydrogels with good biocompatibility are considered safe wound dressings [36]. On day 3, all the experimental groups with hydrogels I–IV added showed a significant proliferation trend than the control group, and there were almost no dead fibroblasts, indicating that hydrogels I–IV had good biocompatibility (Fig. 5A and B). The proliferation of fibroblast is an important factor in promoting skin wound healing [38,39]. We simulated the high levels of glucose and MMP-9 in chronic diabetic wounds and used rat fibroblast L929 cells to evaluate the possibility of hydrogel IV promoting cell proliferation. As shown in Fig. 5C, and D, the cell viability of the hydrogel IV group increased compared with that of the control group in 72 h, probably due to the hydrogel IV composed of chitosan and gelatin simulated the

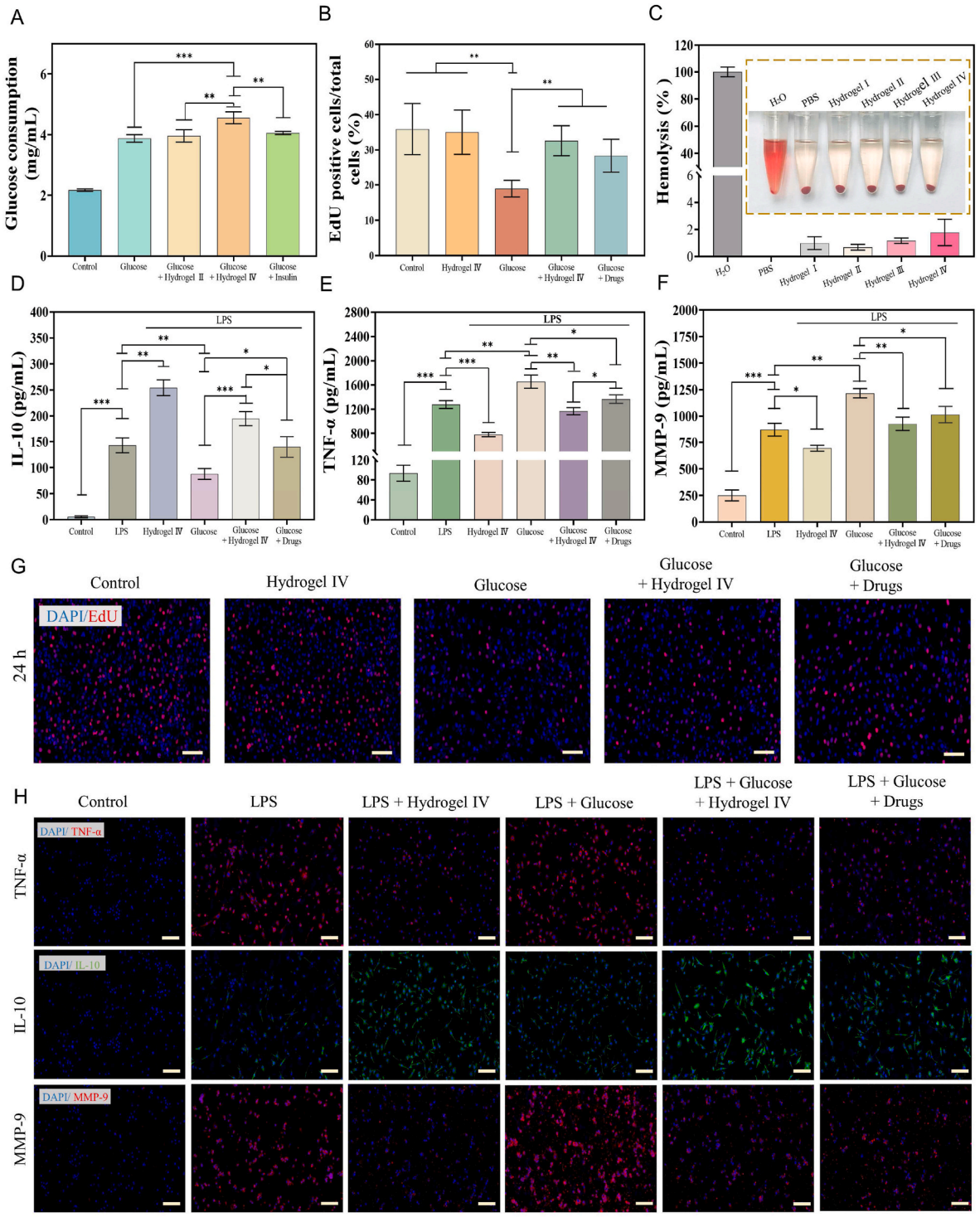

Fig. 6. In vitro properties of the CBP/GMs@Cel&INS hydrogel to promote glucose consumption, cell proliferation, anti-inflammatory. (A) Glucose consumption in L929 cells. (B) Relative amount of EdU positive HUVEC cells. (C) Hemolysis rate of hydrogels. (D, E, F) ELISA for the detection of IL-10, TNF-α, MMP-9. (G) EdU staining of HUVEC cells, scale bar: 200 μm. (H) Immunofluorescence staining of IL-10, TNF-α and MMP-9 in macrophages, scale bar: 100 μm. Note: Hydrogel I: the CBP hydrogel, Hydrogel II: the CBP/GMs hydrogel, Hydrogel III: the CBP/GMs@INS hydrogel, Hydrogel Ⅳ: the CBP/GMs@Cel&INS hydrogel.

extracellular matrix (ECM) [40–42]. The cell viability of fibroblasts cultured with the hydrogel Ⅳ for 72 h in the high levels of glucose and MMP-9 increased by 36.54 ± 7.38% compared with that of the glucose + MMP-9 group, may be attributed to the synergistic effect: insulin was released from the hydrogel Ⅳ through response to the environment, and insulin promotes cell proliferation [43]; the hydrogel IV promoted cell proliferation by being degraded in the high levels of glucose and MMP-9 [42]. Improving migration has also been shown to promote wound healing [36], and insulin stimulates the migration of fibroblasts [44]. The results of the scratch assay and the wound closure rate are shown in Fig. 5E and F. Compared with the control group, the cell mobility of the hydrogel Ⅳ group increased by 30.83 ± 6.19% within 24 h, which may be attributed to the fact that the hydrogel Ⅳ simulated the ECM to promote cell adhesion [42]. At high glucose concentrations (***P < 0.001), the increased migration ability of fibroblasts incubated with hydrogel IV within 24 h may be due to the fact that the hydrogel Ⅳ simulated the ECM while releasing insulin [44]. Celecoxib had no significant effect on the migration of fibroblasts for 24 h, and the small increase of cell mobility in the MMP-9 + hydrogel IV group within 24 h might be added the hydrogel Ⅳ. The increased migration of cells in the MMP-9 + Glucose + Hydrogel Ⅳ group in 24 h was attributed to the synergistic effect of the above reasons, and the hydrogel Ⅳ degraded faster in the high concentration of glucose and MMP-9, which also promoted fibroblasts adhesion and migration [42]. Importantly, compared with the glucose + insulin group, the glucose + hydrogel IV group promoted the migration of fibroblasts in the high concentration of glucose, which might be attributed to the use of hydrogel IV sustained-release insulin, which increased the utilization of insulin which with a short half-life [45]. Furthermore, the migration of fibroblasts in the hydrogel IV group was more significant than that in the control group (**p < 0.01, ***p < 0.001), which showed that hydrogel IV also promoted wound healing when the high levels of glucose and MMP-9 were controlled.

3.6. *In vitro glucose consumption, HUVEC cell proliferation, and anti-inflammatory activities*

Insulin promotes glucose consumption in L929 cells, but insulin with a short half-life has difficulty maintaining long-term high activity [43,46]. The glucose consumption of L929 cells co-cultured with hydrogel Ⅳ for 24 h increased by 17.22 ± 0.12% at 5 mg/mL glucose, while the glucose consumption of L929 cells added with a high concentration of insulin (0.32 mg/mL) increased by only 0.43 ± 0.11%, this fully showed that insulin encapsulated by hydrogel Ⅳ was more active, thus promoting glucose consumption by cells (Fig. 6A and Fig. S4C).

Vascular lesions are also a cause of chronic diabetic wound healing. Hyperglycemia leads to macrovascular and microvascular complications by damaging vascular endothelial cells, resulting in limb ischaemia and loss of sensation, eventually leading to the development of gangrene [47]. Insulin stimulates endothelial cell proliferation by activating the Ras-MAPK (mitogen-activated protein kinase) cascade, thereby promoting angiogenesis [48]. To demonstrate that insulin effectively released from hydrogel IV promotes endothelial cell proliferation, HUVECs were treated with EdU to evaluate the early phase of cell cycle progression [40]. S phase cells in the control group, hydrogel IV group, glucose group, glucose + hydrogel IV group, and glucose + drugs (insulin and celecoxib) groups were 35.9 ± 7.26%, 35.05 ± 6.28%, 18.96 ± 2.35%, 32.62 ± 4.25%, and 28.39 ± 4.66%, respectively (Fig. 6B and G). The results showed that high levels of glucose significantly reduced the number of HUVECs entering the proliferative phase, and the insulin effectively released by hydrogel IV promoted the transformation of G0/G1, thus fully improving the viability of HUVEC cell proliferation. In addition, the hemolysis rates of hydrogels I-IV were 0.99 ± 0.47%, 0.7 ± 0.21%, 1.18 ± 0.19%, and 1.79 ± 0.98% (Fig. 6C), and excellent blood compatibility ensured the possibility of hydrogels as wound dressings.

Early in wound healing, inflammatory cells secrete several key inflammatory cytokines to promote local or systemic defence responses, which are critical for wound healing [36]. However, chronic diabetic wounds are in the long-term inflammatory phase due to macrophage dysfunction, which hinders the development of damaged tissue to the proliferation and remodelling phase of wound healing [9,13], and the high expression of MMP-9 in chronic diabetic wounds was also an important reason for the non-healing [15]. To simulate chronic inflammation and oversecretion of MMP-9 in chronic diabetic wounds, LPS was used to induce macrophages (RAW264.7) to secrete inflammatory factors and MMP-9 via the 3 mitogen-activated protein kinase (MAPK) pathways and the NF-κ B signalling pathway [20,49,50]. ELISA was used to quantify the secretion of pro-inflammatory cytokines (TNF-α), anti-inflammatory cytokines (IL-10), and MMP-9 to demonstrate the anti-inflammatory ability of hydrogel IV. Fig. 6D and E shows that the secretion of TNF-α by LPS-induced RAW264.7 cells was increased by 29.52 ± 3.76% and IL-10 was down-regulated by 38.74 ± 5.55% under high levels of glucose. Persistent hyperglycemia was the most significant biochemical characteristic of diabetes, which indicated that chronic diabetic wounds were more prone to long-term inflammation. After treatment with hydrogel Ⅳ, the secretion of TNF-α and IL-10 in LPS-induced RAW264.7, which were injured by high concentrations of glucose, decreased by 29.38 ± 2.30% and increased by 121.46 ± 11.42%, indicating that hydrogel IV had excellent anti-inflammatory properties due to the effective release of the anti-inflammatory drug (celecoxib). As shown in Fig. 6F, MMP-9 was secreted by RAW264.7 cells in the glucose, glucose + hydrogel Ⅳ, and glucose + drugs (insulin and celecoxib) group at 1215.98 ± 43.96 pg/mL, 927.43 ± 64.08 pg/mL, 1015.47 ± 76.8 pg/mL, indicating that hydrogel IV could reduce the oversecretion of MMP-9. TNF-α promotes the expression of MMP-9 through the NF-κ B pathway [45]; therefore, high levels of glucose might promote the secretion of MMP-9 by increasing the expression of TNF-α, and the downregulation of MMP-9 might be attributed to the anti-inflammatory ability of hydrogel Ⅳ. In addition, the anti-inflammatory effect of the hydrogel-treated group was superior to that of the drug-treated group, which might be due to the higher cell utilization rate of hydrophobic celecoxib through the encapsulation of hydrogel IV. Finally, immunofluorescence staining was used to detect TNF-α, IL-10, and MMP-9 in RAW264.7 cells (Fig. 6H). Immunofluorescence staining of the merge of TNF-α and IL-10 were shown in Fig. S4D. All the above results showed that hydrogel IV decreased the expression of TNF-α, enhanced the expression of IL-10, and decreased the expression of MMP-9, which was consistent with the results shown in Fig. 6D–F.

3.7. *Skin wound healing of diabetic rats*

Hydrogels are widely used as wound dressings for the skin, which provide a moist environment and accelerate tissue repair [63–65]. STZ can destroy the pancreatic β-cells of rats after a single injection of high dose, which inhibits insulin synthesis and release and induces type I diabetes [23]. Therefore, this study used full-thickness wounds in STZ-induced diabetic rats to evaluate the efficacy of hydrogels in helping diabetic wound healing. As shown in Fig. 7C and supplementary video, the CBP/GMs@Cel&INS hydrogel showed good injectable ability, and the new granulation of the wound was not damaged when the hydrogel was removed. In addition, the hydrogels showed strong adhesion to follow the movement of rat wounds without falling off (supplementary video). In summary, the CBP/GMs@Cel&INS hydrogel has the advantages of shape adaptation, injectability, strong adhesion, and strippability, which makes it convenient for clinical applications. The wound of the gauze control group and the commercial hydrogel control group were treated with gauze and commercial hydrogel (HeraDerm®) respectively, the properties of hydrogel II–IV to promote wound healing were evaluated (Fig. 7B). As shown in Fig. S5B, all SD rats maintained stable hyperglycemia (blood glucose >300 mg/dL) before wound formation. On day 7, there was redness and swelling

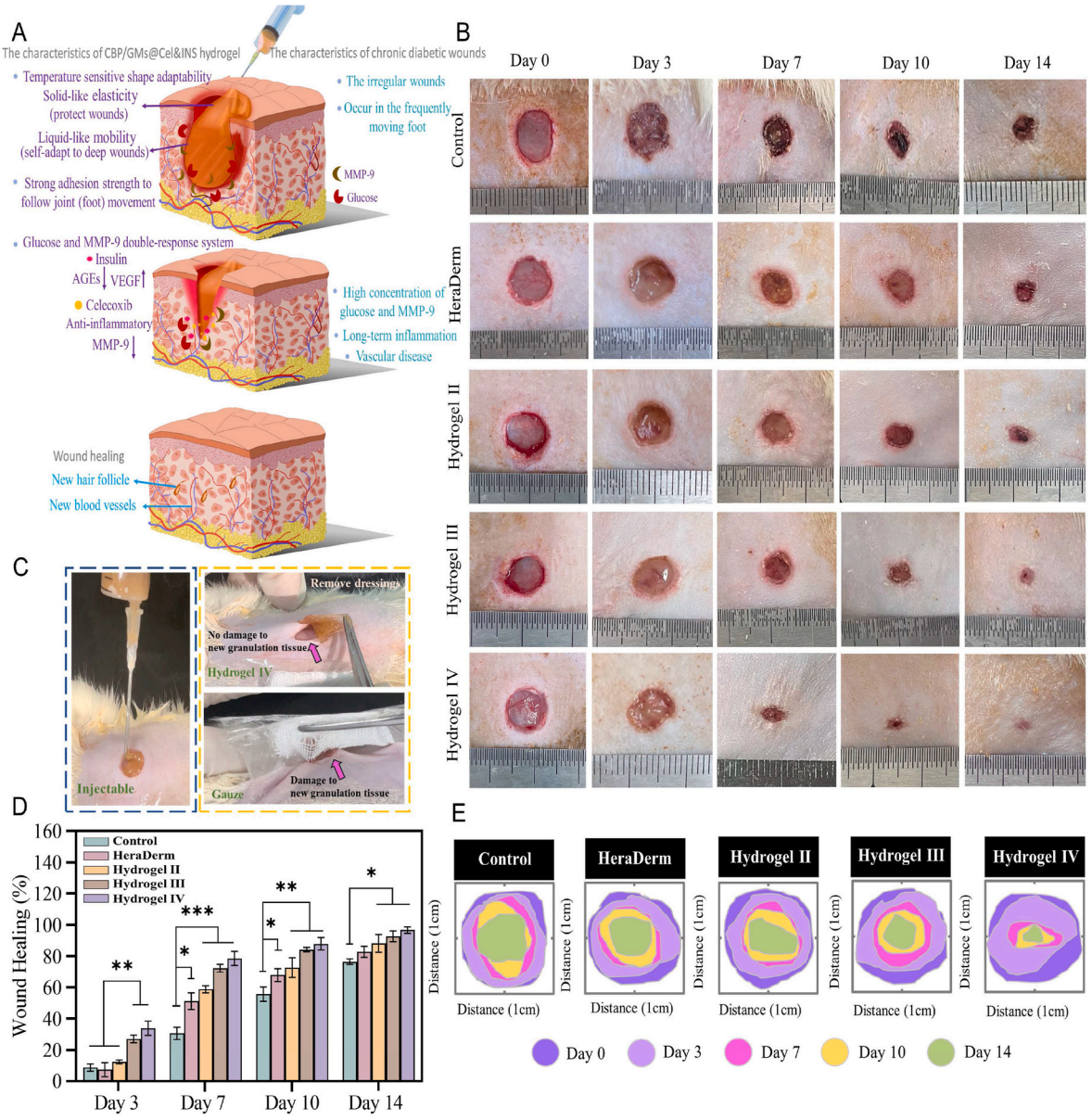

Fig. 7. Analysis of skin wound healing in diabetic rats. (A) Mechanism of wound healing induced by CBP/GMs@Cel&INS hydrogel. (B) Photos of the wounds at days 0, 3, 7, 10, 14. (C) Photographs of injection and stripping of hydrogels, and the adhesion of gauze to wounds during stripping. (D) Wound healing rate at days 3, 7, 10, 14. (E) Analysis of wound healing trace on days 0, 3, 7, 10, 14. Note: Hydrogel II: the CBP/GMs hydrogel; Hydrogel III: the CBP/GMs@INS hydrogel; Hydrogel Ⅳ: the CBP/GMs@Cel&INS hydrogel.

around the wounds treated with gauze and the HeraDerm hydrogel; however, the hydrogel IV group had almost no swelling or redness. Long-term inflammation is one of the main causes of difficulty in healing chronic diabetic wounds. The results showed that hydrogel IV could reduce wound inflammation, which was related to the long-term release of insulin and celecoxib in hydrogel IV. Wound healing was statistically analysed (Figs. 7D, E, and S5A). On day 7, the wound areas of the hydrogel III–IV group were significantly smaller than that of the gauze control group and the HeraDerm group, and the hydrogel Ⅳ-treated wounds were also smaller at day 7 than those in some previous studies [51–54]. On day 10, the wound contraction of the hydrogel II group was about 4.84 ± 2.19% higher than that of the HeraDerm group, while the wound healing rate of the hydrogel IV group surpassed approximately 20.1 ± 2.48% of that of the HeraDerm group, indicating that the release system of hydrogel Ⅳ could release insulin and celecoxib effective in wounds, and hydrogel II containing CS and gelatin can also promote wound healing. On day 14, the wound contraction of the gauze and the HeraDerm groups was 76.63 ± 1.73% and 82.87 ± 3.46%, and the wound healing rate of the hydrogel Ⅳ group was 96.68 ± 2.04%, the results showed that the hydrogel Ⅳ was more effective in accelerating wound healing than commercial hydrogels. In summary, the healing time of the gauze group was longer than 18 days, and hydrogel IV reduced the wound healing time to 14 days and had an excellent therapeutic effect and convenient clinical application during the whole wound healing process.

Supplementary video related to this article can be found at https://doi.org/10.1016/j.bioactmat.2022.01.004

3.8. Histological evaluation of wound regeneration

Histological evaluation revealed the treatment effect of the hydrogel on chronic wounds of diabetes by clarifying the healing process of regenerated tissue. HE staining was performed on days 7 and 14 to evaluate wound healing (Fig. 8A), and the results of HE staining in normal

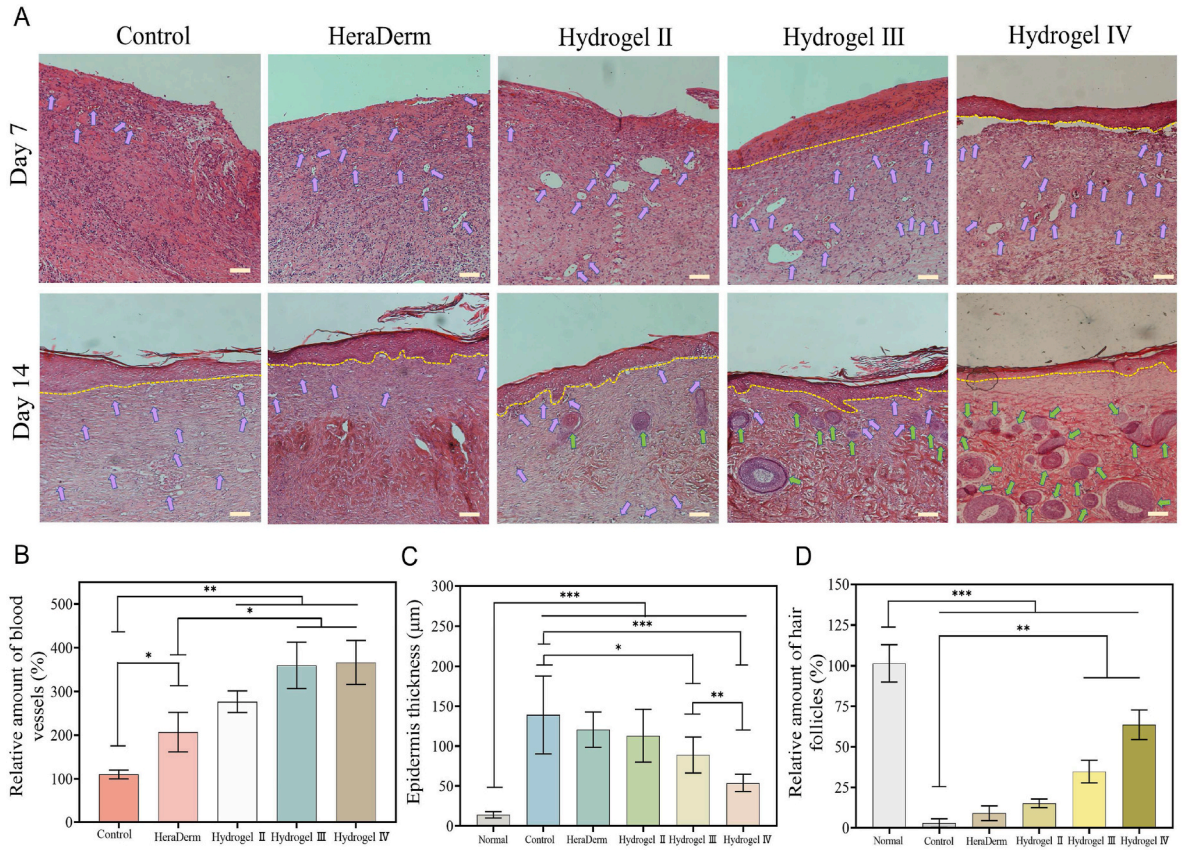

Fig. 8. Analysis of wound healing process. (A) H&E stain image of regenerated skin tissue, 100 μm on the scale (yellow dotted line denoted epithelial-dermal boundary, purple arrows denoted capillaries, and green arrows denoted hair follicles), scale bar: 100 μm. (B) Capillary densities density of granulation tissue under different treatments, data were normalised against the results of the gauze group at day 7, and the data of the gauze group was defined as 100%. (C) Epithelial thickness of granulation tissues following different treatments at day 14. (D) Hair follicle density of regenerated skin tissues in each group on day 14, data were normalised against the normal skin tissues of diabetic rats at day 14, and the data of the normal skin tissues was defined as 100%. Note: Hydrogel II: the CBP/GMs hydrogel; Hydrogel III: the CBP/GMs@INS hydrogel; Hydrogel Ⅳ: the CBP/GMs@Cel&INS hydrogel.

skin tissue of diabetic rats are shown in Fig. S5C. On day 7, significant inflammatory cells infiltrating the granulation tissue were observed in the gauze, HeraDerm, and the wounds of hydrogel III and hydrogel IV groups contained fewer inflammatory cells and formed epithelial layers. This was attributed to the release of insulin from the hydrogel III and hydrogel Ⅳ in response to high levels of glucose around chronic diabetic wounds. Insulin accelerated wound healing by promoting the proliferation, migration, and secretion of keratinocytes, endothelial cells, and fibroblasts [44,55]; also, insulin reduced the inflammation, caused by PI3K/Akt/Rac-1 and PPAR-γ pathways [56]. In addition, hydrogel IV released celecoxib in response to high concentrations of MMP-9, shortening the inflammatory stage of wounds. As shown in Fig. 8B, the capillary density of the wounds in each group was quantitatively analysed on day 7. The hydrogel III and hydrogel IV groups had more new blood vessels, which was attributed to the promotion of cell proliferation and migration by hydrogels III–IV, and the long-term release of insulin promoted angiogenesis [57]. Re-epithelialisation is the thinning and maturation of epithelial structures and is an important stage of skin regeneration. From 7 days to 14 days, the epithelial thickness of hydrogel III and the hydrogel Ⅳ groups tended to be thinner in the healing process, and on day 14, each group formed epithelial structures. The epithelium thickness of the hydrogel IV group was the thinnest and similar to that of the normal group, while the other groups had significantly thicker epithelium (Fig. 8C). In addition, hair follicles were used to evaluate the integrity of tissue regeneration as an important functional skin structure. On day 14, the density of hair follicles in the hydrogel IV group was significantly higher than that in the other groups (Fig. 8D and Fig. S5C), suggesting that glucose and MMP-9 dual-response thermosensitive shape self-adaptive hydrogel could effectively accelerate the healing of chronic diabetic wounds.

3.9. Pre-healing factor analysis

To further study the mechanism by which the CBP@Cel&INS hydrogel promoted wound healing, the typical pre-healing factors were analysed. The typical chronic diabetic wound was in the inflammation phase for a long time [11,13]. As the typical pro-inflammatory cytokine and the anti-inflammatory cytokine, TNF-α and IL-10 were important indicators of inflammatory response during the early healing phase [8], on day 7 (the phase of inflammation in naturally healing chronic diabetic wounds), compared with the gauze group and the HeraDerm group, the concentration of TNF-α increased and the concentration of IL-10 decreased in the hydrogel III group, and the highest levels of IL-10 and almost no levels of TNF-α were detected in hydrogel IV treated wounds, suggesting that the anti-inflammatory effect of hydrogel III was limited, and hydrogel Ⅳ had excellent anti-inflammatory properties (Fig. 9A, B, and C). The anti-inflammatory effect of hydrogel III might be due to the effective release of insulin, and the anti-inflammatory effect of hydrogel IV was mainly attributed to the long-term release of celecoxib in the wound on-demand. In addition, the Maillard reaction caused by continuous hyperglycemia in diabetic patients promoted the accumulation of advanced glycation end products (AGEs), which is also an important factor in chronic diabetic wound non-healing [51]. AGEs in skin collagen are directly related to long-term glucose control [58], and topical application of insulin to wounds could reduce the accumulation of AGEs [59]. On day 7, fewer AGEs accumulated in hydrogels III and IV

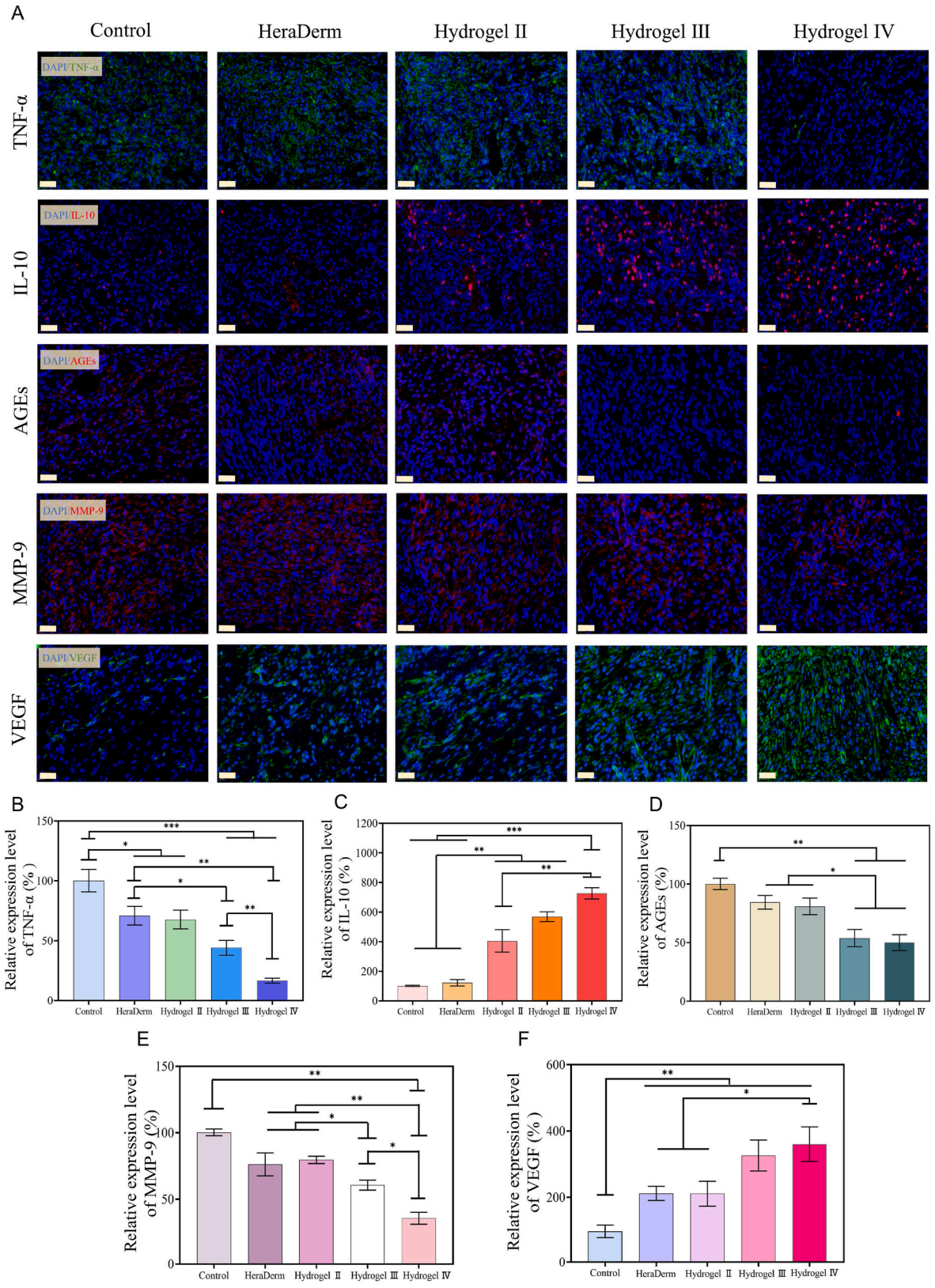

Fig. 9. Immunofluorescence staining analysis of Pre-healing factor. (A) On day 7, immunofluorescence staining of TNF-α, IL-10, AGEs, MMP-9, and VEGF was performed on the wounds of different groups, scale bar: 20 μm. (B, C, D, E, F) The relative quantitative analysis of the expression of TNF-α, IL-10, AGEs, MMP-9, and VEGF data were normalised against the results of the gauze group at day 7, and the data of the gauze group was defined as 100%. Note: Hydrogel II: the CBP/GMs hydrogel; Hydrogel III: the CBP/GMs@INS hydrogel; Hydrogel Ⅳ: the CBP/GMs@Cel&INS hydrogel.

than that in the other groups (Fig. 9A and D), suggesting that hydrogels III and IV were effective in the release of insulin, and hydrogel Ⅳ could also reduce the accumulation of AGEs via excellent anti-inflammatory effect [60]. Moreover, many studies have shown that sustained high concentrations of pro-inflammatory cytokines and AGEs induce high expression of MMPs in chronic diabetic wounds [9,61,62], while the oversecretion of MMP-9 continuously degrades various growth factors and extracellular matrix (ECM) required for wound healing, which is not conducive to the healing of chronic diabetic wounds. On day 7, a lower concentration of MMP-9 was detected in wounds of the hydrogel IV group (Fig. 9A and E); therefore, the more effective reduction of MMP-9 in the hydrogel IV group might be attributed to the hydrogel IV effectively releasing insulin and celecoxib. Furthermore, the proliferation and activity of vascular endothelial cells and fibroblasts were reduced due to the damage of vascular endothelial cells by AGEs and the degradation of ECM by oversecretion of MMP-9, resulting in the destruction of peripheral vasculature and the reduction of new blood vessels, which reduces the nutrient supply of new granulation tissues and prolongs the wound healing time. VEGF was included as an important indicator to evaluate the ability of wound dressings to promote angiogenesis. On day 7, the secretion of VEGF in hydrogel IV was the highest, followed by hydrogel III (Fig. 9A and F). This was due to insulin in hydrogel III and hydrogel IV was sensitively released at high levels of glucose, which promoted the secretion of VEGF through the PI3K/AKT pathway [48,57], and the lower secretion of MMP-9 in wounds of the hydrogel IV group reduced the damage to the viability of vascular endothelial cells. These results indicate that the CBP/GMs@Cel&INS hydrogel promoted chronic diabetic wound healing by exerting anti-inflammatory effects, reducing the accumulation of AGEs and the oversecretion of MMP-9, upregulating the secretion of VEGF, and promoting angiogenesis.

4. Conclusion

In summary, this study prepared a glucose and MMP-9 dual-response temperature-sensitive shape-adaptive hydrogel (CBP@GMs/Cel&INS) for the treatment of chronic diabetic wounds. When CBP@GMs/Cel&INS was exposed to wounds, on the one hand, the thermosensitive adaptability of the hydrogel ensured that quickly adapt to deep wounds and provided mechanical properties to protect wounds; on the other hand, CBP@GMs/Cel&INS on-demand released insulin and the anti-inflammatory drug (celecoxib) under the special wound environment of high concentrations glucose and MMP-9 in chronic diabetic wounds, CBP@GMs/Cel&INS promoted chronic diabetic wound healing more efficiently through the synergistic effect of glucose and MMP-9 dual response system and temperature-sensitive adaptation. In addition, CBP@GMs/Cel&INS with excellent remodeling, adaptability, and enhanced adhesion strength fitted the wound completely, thus reducing the risk of wound infection and improving the efficiency of drug release, while rapid self-healing prolonged the service life of the hydrogel. CBP@GMs/Cel&INS composed of CS, gelatin, and PVA had excellent biocompatibility and effectively promoted cell proliferation and migration, effectively releasing insulin and celecoxib, thus exerting anti-inflammatory, hypoglycaemic, and promoting angiogenesis. In a full-thickness skin defect model of diabetic rats, wounds treated with CBP@GMs/Cel&INS healed faster than those treated with other groups with the most idealized epithelial structure and angiogenesis along with hair follicle regeneration. Further mechanistic studies showed that CBP@GMs/Cel&INS down-regulated the expression of inflammatory cytokines and downstream MMP9, down-regulated the expression of AGEs, and accelerated angiogenesis, thus having significant therapeutic effects on chronic diabetic wounds. These results suggest that CBP@GMs/Cel&INS is a promising wound dressing for chronic diabetic wounds.

CRediT authorship contribution statement

Wanyi Zhou: Methodology, Validation, Formal analysis, Investigation, Data curation, Writing – original draft. **Zhiguang Duan:** Methodology, Software. **Rongzhan Fu:** Methodology, Investigation. **Chenhui Zhu:** Conceptualization, Methodology, Writing – review & editing, Project administration, Funding acquisition. **Daidi Fan:** Conceptualization, Methodology, Writing – review & editing, Project administration, Funding acquisition.

Declaration of competing interest

The authors declare that they have no known competing financial interests or personal relationships that could have appeared to influence the work reported in this paper.

Acknowledgements

This work was supported by the National key Research and development program of China (2019YFA0905200), the National Natural Science Foundation of China (21878247, 21808184), and Key Program of the National Natural Science Foundation of China (21838009).

Appendix A. Supplementary data

Supplementary data to this article can be found online at https://doi.org/10.1016/j.bioactmat.2022.01.004.

References

[1] N.S. El-Salamouni, M.A. Gowayed, N.L. Seiffein, R.A. Abdel-Moneim, M.A. Kamel, G.S. Labib, Valsartan solid lipid nanoparticles integrated hydrogel: a challenging repurposed use in the treatment of diabetic foot ulcer, in-vitro/in-vivo experimental study, Int. J. Pharm. 592 (2021) 120091.
[2] M. Yovera-Aldana, S. Saenz-Bustamante, Y. Quispe-Landeo, R. Aguero-Zamora, J. Salcedo, C. Sarria, N. Gonzales-Grandez, M. Briceno-Alvarado, A. Antezana-Roman, H. Manrique, D.G. Armstrong, Nationwide prevalence and clinical characteristics of inpatient diabetic foot complications: a Peruvian multicenter study, Primary Care Diabetes 15 (3) (2021) 480–487.
[3] V. Falanga, Chronic wounds: pathophysiologic and experimental considerations, J. Invest. Dermatol. 100 (5) (1993) 721–725.
[4] R. Lobmann, A. Ambrosch, G. Schultz, K. Waldmann, S. Schiweck, H. Lehnert, Expression of matrix-metalloproteinases and their inhibitors in the wounds of diabetic and non-diabetic patients, Diabetologia 45 (7) (2002) 1011–1016.
[5] B. Akinci, C. Terzi, G. Sevindik, F. Yuksel, U.A. Tunc, S. Tunali, S. Yesil, Hyperglycemia is associated with lower levels of urokinase-type plasminogen activator and urokinase-type plasminogen activator receptor in wound fluid, J. Diabetes Complicat. 28 (6) (2014) 844–849.
[6] S.W. Hyun, J. Kim, K. Jo, J.S. Kim, C.S. Kim, Aster koraiensis extract improves impaired skin wound healing during hyperglycemia, Integr. Med. Res. 7 (4) (2018) 351–357.
[7] N. Li, L. Yang, C. Pan, P.E. Saw, M. Ren, B. Lan, J. Wu, X. Wang, T. Zeng, L. Zhou, L. M. Zhang, C. Yang, L. Yan, Naturally-occurring bacterial cellulose-hyperbranched cationic polysaccharide derivative/MMP-9 siRNA composite dressing for wound healing enhancement in diabetic rats, Acta Biomater. 102 (2020) 298–314.
[8] J. Sonamuthu, Y. Cai, H. Liu, M.S.M. Kasim, V.R. Vasanthakumar, B. Pandi, H. Wang, J. Yao, MMP-9 responsive dipeptide-tempted natural protein hydrogel-based wound dressings for accelerated healing action of infected diabetic wound, Int. J. Biol. Macromol. 153 (2020) 1058–1069.
[9] J. Liu, Z. Chen, J. Wang, R. Li, T. Li, M. Chang, F. Yan, Y. Wang, Encapsulation of curcumin nanoparticles with MMP9-responsive and thermos-sensitive hydrogel improves diabetic wound healing, ACS Appl. Mater. Interfaces 10 (19) (2018) 16315–16326.
[10] H. Yaseen, M. Khamaisi, Skin well-being in diabetes: role of macrophages, Cell. Immunol. 356 (2020) 104154.
[11] Moganti, F. Li, C. Schmuttermaier, S. Riemann, H. Kluter, A. Gratchev, M. C. Harmsen, J. Kzhyshkowska, Hyperglycemia induces mixed M1/M2 cytokine profile in primary human monocyte-derived macrophages, Immunobiology 222 (10) (2017) 952–959.
[12] K. Itatsu, M. Sasaki, J. Yamaguchi, S. Ohira, A. Ishikawa, H. Ikeda, Y. Sato, K. Harada, Y. Zen, H. Sato, T. Ohta, M. Nagino, Y. Nimura, Y. Nakanuma, Cyclooxygenase-2 is involved in the up-regulation of matrix metalloproteinase-9 in cholangiocarcinoma induced by tumor necrosis factor-alpha, Am. J. Pathol. 174 (3) (2009) 829–841.
[13] B. Hu, M. Gao, K.O. Boakye-Yiadom, W. Ho, W. Yu, X. Xu, X.Q. Zhang, An intrinsically bioactive hydrogel with on-demand drug release behaviors for diabetic wound healing, Bioact. Mater. 6 (12) (2021) 4592–4606.

[14] T.T. Nguyen, D. Ding, W.R. Wolter, M.M. Champion, D. Hesek, M. Lee, R.L. Perez, V.A. Schroeder, M.A. Suckow, S. Mobashery, M. Chang, Expression of active matrix metalloproteinase-9 as a likely contributor to the clinical failure of aclerastide in treatment of diabetic foot ulcers, Eur. J. Pharmacol. 834 (2018) 77–83.

[15] T.T. Nguyen, D. Ding, W.R. Wolter, R.L. Perez, M.M. Champion, K.V. Mahasenan, D. Hesek, M. Lee, V.A. Schroeder, J.I. Jones, E. Lastochkin, M.K. Rose, C. E. Peterson, M.A. Suckow, S. Mobashery, M. Chang, Validation of matrix metalloproteinase-9 (MMP-9) as a novel target for treatment of diabetic foot ulcers in humans and discovery of a potent and selective small-molecule MMP-9 inhibitor that accelerates healing, J. Med. Chem. 61 (19) (2018) 8825–8837.

[16] N. Malekpour Alamdari, A. Shafiee, A. Mirmohseni, S. Besharat, Evaluation of the efficacy of platelet-rich plasma on healing of clean diabetic foot ulcers: a randomized clinical trial in Tehran, Iran, Diabetes Metab. Syndr. Clin. Res. Rev. 15 (2) (2021) 621–626.

[17] N. Parizad, K. Hajimohammadi, R. Goli, Surgical debridement, maggot therapy, negative pressure wound therapy, and silver foam dressing revive hope for patients with diabetic foot ulcer: a case report, Int. J. Surg. Case Rep. 82 (2021) 105931.

[18] N. Kobyliak, L. Abenavoli, L. Kononenko, D. Kyriienko, M. Spivak, Neuropathic diabetic foot ulcers treated with cerium dioxide nanoparticles: a case report, Diabetes Metab. Syndr. Clin. Res. Rev. 13 (1) (2019) 228–234.

[19] H. Lei, D. Fan, Conductive, adaptive, multifunctional hydrogel combined with electrical stimulation for deep wound repair, Chem. Eng. J. 421 (2021).

[20] C. Hu, F. Zhang, L. Long, Q. Kong, R. Luo, Y. Wang, Dual-responsive injectable hydrogels encapsulating drug-loaded micelles for on-demand antimicrobial activity and accelerated wound healing, J. Contr. Release 324 (2020) 204–217.

[21] F. Qian, Y. Han, Z. Han, D. Zhang, L. Zhang, G. Zhao, S. Li, G. Jin, R. Yu, H. Liu, In Situ implantable, post-trauma microenvironment-responsive, ROS Depletion Hydrogels for the treatment of Traumatic brain injury, Biomaterials 270 (2021) 120675.

[22] K.S. Oh, C. Hwang, H.Y. Lee, J.S. Song, H.J. Park, C.K. Lee, I. Song, T.H. Lim, Preclinical studies of ropivacaine extended-release from a temperature responsive hydrogel for prolonged relief of pain at the surgical wound, Int. J. Pharm. 558 (2019) 225–230.

[23] L. Zhao, L. Niu, H. Liang, H. Tan, C. Liu, F. Zhu, pH and glucose dual-responsive injectable hydrogels with insulin and fibroblasts as bioactive dressings for diabetic wound healing, ACS Appl. Mater. Interfaces 9 (43) (2017) 37563–37574.

[24] R. Laurano, M. Boffito, M. Abrami, M. Grassi, A. Zoso, V. Chiono, G. Ciardelli, Dual stimuli-responsive polyurethane-based hydrogels as smart drug delivery carriers for the advanced treatment of chronic skin wounds, Bioact. Mater. 6 (9) (2021) 3013–3024.

[25] Y. Li, X. Wang, Y.N. Fu, Y. Wei, L. Zhao, L. Tao, Self-adapting hydrogel to improve the therapeutic effect in wound-healing, ACS Appl. Mater. Interfaces 10 (31) (2018) 26046–26055.

[26] H.M. Yang, C.W. Park, K.W. Lee, Enhanced surface decontamination of radioactive Cs by self-generated, strippable hydrogels based on reversible cross-linking, J. Hazard Mater. 362 (2019) 72–81.

[27] R. Yang, X. Liu, Y. Ren, W. Xue, S. Liu, P. Wang, M. Zhao, H. Xu, B. Chi, Injectable adaptive self-healing hyaluronic acid/poly (gamma-glutamic acid) hydrogel for cutaneous wound healing, Acta Biomater. 127 (2021) 102–115.

[28] H.-M. Yang, C.W. Park, K.W. Lee, B.-S. Lee, I. Kim, I.-H. Yoon, Polyvinyl alcohol-borate hydrogel containing Prussian blue for surface decontamination, J. Radioanal. Nucl. Chem. 316 (3) (2018) 955–962.

[29] C. Ancla, V. Lapeyre, I. Gosse, B. Catargi, V. Ravaine, Designed glucose-responsive microgels with selective shrinking behavior, Langmuir 27 (20) (2011) 12693–12701.

[30] J. Qu, X. Zhao, Y. Liang, T. Zhang, P.X. Ma, B. Guo, Antibacterial adhesive injectable hydrogels with rapid self-healing, extensibility and compressibility as wound dressing for joints skin wound healing, Biomaterials 183 (2018) 185–199.

[31] J. Li, W. Hu, Y. Zhang, H. Tan, X. Yan, L. Zhao, H. Liang, pH and glucose dually responsive injectable hydrogel prepared by in situ crosslinking of phenylboronic modified chitosan and oxidized dextran, J. Polym. Sci. Polym. Chem. 53 (10) (2015) 1235–1244.

[32] S. Li, N. Chen, X. Li, Y. Li, Z. Xie, Z. Ma, J. Zhao, X. Hou, X. Yuan, Bioinspired double-dynamic-bond crosslinked bioadhesive enables post-wound closure care, Adv. Funct. Mater. 30 (17) (2020).

[33] B. Balakrishnan, D. Soman, U. Payanam, A. Laurent, D. Labarre, A. Jayakrishnan, A novel injectable tissue adhesive based on oxidized dextran and chitosan, Acta Biomater. 53 (2017) 343–354.

[34] J.L. Daristotle, S.T. Zaki, L.W. Lau, O.B. Ayyub, M. Djouini, P. Srinivasan, M. Erdi, A.D. Sandler, P. Kofinas, Pressure-sensitive tissue adhesion and biodegradation of viscoelastic polymer blends, ACS Appl. Mater. Interfaces 12 (14) (2020) 16050–16057.

[35] M. Diba, W.A. Camargo, M. Brindisi, K. Farbod, A. Klymov, S. Schmidt, M. J. Harrington, L. Draghi, A.R. Boccaccini, J.A. Jansen, J.J.J.P. van den Beucken, S. C.G. Leeuwenburgh, Composite colloidal gels made of bisphosphonate-functionalized gelatin and bioactive glass particles for regeneration of osteoporotic bone defects, Adv. Funct. Mater. 27 (45) (2017).

[36] Y. Yuan, S. Shen, D. Fan, A physicochemical double cross-linked multifunctional hydrogel for dynamic burn wound healing: shape adaptability, injectable self-healing property and enhanced adhesion, Biomaterials 276 (2021) 120838.

[37] J. Yang, C.-R. Han, X.-M. Zhang, F. Xu, R.-C. Sun, Cellulose nanocrystals mechanical reinforcement in composite hydrogels with multiple cross-links: correlations between dissipation properties and deformation mechanisms, Macromolecules 47 (12) (2014) 4077–4086.

[38] C.R. Kruse, M. Singh, J.A. Sorensen, E. Eriksson, K. Nuutila, The effect of local hyperglycemia on skin cells in vitro and on wound healing in euglycemic rats, December, J. Surg. Res. 206 (2) (2016) 418–426.

[39] I. Kurt-Celep, E. Celep, S. Akyuz, Y. Inan, T.H. Barak, G. Akaydin, D. Telci, E. Yesilada, Hypericum olympicum L. recovers DNA damage and prevents MMP-9 activation induced by UVB in human dermal fibroblasts, J. Ethnopharmacol. 246 (2020) 112202.

[40] S. Shen, D. Fan, Y. Yuan, X. Ma, J. Zhao, J. Yang, An ultrasmall infinite coordination polymer nanomedicine-composited biomimetic hydrogel for programmed dressing-chemo-low level laser combination therapy of burn wounds, Chem. Eng. J. 426 (2021).

[41] M. Mekhail, K. Jahan, M. Tabrizian, Genipin-crosslinked chitosan/poly-L-lysine gels promote fibroblast adhesion and proliferation, Carbohydr. Polym. 108 (2014) 91–98.

[42] Q. Sun, Y. Hou, Z. Chu, Q. Wei, Soft overcomes the hard: flexible materials adapt to cell adhesion to promote cell mechanotransduction, Bioact. Mater. 10 (2022) 397–404.

[43] P. Kaur, A.K. Sharma, D. Nag, A. Das, S. Datta, A. Ganguli, V. Goel, S. Rajput, G. Chakrabarti, B. Basu, D. Choudhury, Novel nano-insulin formulation modulates cytokine secretion and remodeling to accelerate diabetic wound healing, Nanomedicine 15 (1) (2019) 47–57.

[44] M.H. Lima, A.M. Caricilli, L.L. de Abreu, E.P. Araujo, F.F. Pelegrinelli, A. C. Thirone, D.M. Tsukumo, A.F. Pessoa, M.F. dos Santos, M.A. de Moraes, J. B. Carvalheira, L.A. Velloso, M.J. Saad, Topical insulin accelerates wound healing in diabetes by enhancing the AKT and ERK pathways: a double-blind placebo-controlled clinical trial, PLoS One 7 (5) (2012), e36974.

[45] A. Ehterami, M. Salehi, S. Farzamfar, A. Vaez, H. Samadian, H. Sahrapeyma, M. Mirzaii, S. Ghorbani, A. Goodarzi, In vitro and in vivo study of PCL/COLL wound dressing loaded with insulin-chitosan nanoparticles on cutaneous wound healing in rats model, Int. J. Biol. Macromol. 117 (2018) 601–609.

[46] M.C. Ribeiro, V.L.R. Correa, F. Silva, A.A. Casas, A.L.D. Chagas, L.P. Oliveira, M. P. Miguel, D.G.A. Diniz, A.C. Amaral, L.B. Menezes, Wound healing treatment using insulin within polymeric nanoparticles in the diabetes animal model, Eur. J. Pharmaceut. Sci. 150 (2020) 105330.

[47] S. Paul, A. Ali, R. Katare, Molecular complexities underlying the vascular complications of diabetes mellitus-A comprehensive review, J. Diabetes Complicat. 34 (8) (2020) 107613.

[48] Z.Y. Jiang, Z. He, B.L. King, T. Kuroki, D.M. Opland, K. Suzuma, I. Suzuma, K. Ueki, R.N. Kulkarni, C.R. Kahn, G.L. King, Characterization of multiple signaling pathways of insulin in the regulation of vascular endothelial growth factor expression in vascular cells and angiogenesis, J. Biol. Chem. 278 (34) (2003) 31964–31971.

[49] H.J. Choi, T.W. Chung, J.E. Kim, H.S. Jeong, M. Joo, J. Cha, C.H. Kim, K.T. Ha, Aesculin inhibits matrix metalloproteinase-9 expression via p38 mitogen activated protein kinase and activator protein 1 in lipopolysachride-induced RAW264.7 cells, Int. Immunopharm. 14 (3) (2012) 267–274.

[50] R.T. de Pinho, W.S. da Silva, L.M. de Castro Cortes, P. da Silva Vasconcelos Sousa, R.O. de Araujo Soares, C.R. Alves, Production of MMP-9 and inflammatory cytokines by Trypanosoma cruzi-infected macrophages, Exp. Parasitol. 147 (2014) 72–80.

[51] H.J. Kang, S. Kumar, A. D'Elia, B. Dash, V. Nanda, H.C. Hsia, M.L. Yarmush, F. Berthiaume, Self-assembled elastin-like polypeptide fusion protein coacervates as competitive inhibitors of advanced glycation end-products enhance diabetic wound healing, J. Contr. Release 333 (2021) 176–187.

[52] J. Zhu, G. Jiang, W. Hong, Y. Zhang, B. Xu, G. Song, T. Liu, C. Hong, L. Ruan, Rapid gelation of oxidized hyaluronic acid and succinyl chitosan for integration with insulin-loaded micelles and epidermal growth factor on diabetic wound healing, Mater. Sci. Eng. C 117 (2020) 111273.

[53] W. Pan, X. Qi, Y. Xiang, S. You, E. Cai, T. Gao, X. Tong, R. Hu, J. Shen, H. Deng, Facile formation of injectable quaternized chitosan/tannic acid hydrogels with antibacterial and ROS scavenging capabilities for diabetic wound healing, Int. J. Biol. Macromol. 195 (2022) 190–197.

[54] Y. Zhang, Y. Zheng, F. Shu, R. Zhou, B. Bao, S. Xiao, K. Li, Q. Lin, L. Zhu, Z. Xia, In situ-formed adhesive hyaluronic acid hydrogel with prolonged amnion-derived conditioned medium release for diabetic wound repair, Carbohydr. Polym. 276 (2022) 118752.

[55] M.K. Bhettani, M. Rehman, H.N. Altaf, O.S. Altaf, Effectiveness of topical insulin dressings in management of diabetic foot ulcers, World J. Surg. 44 (6) (2020) 2028–2033.

[56] T. Yu, M. Gao, P. Yang, D. Liu, D. Wang, F. Song, X. Zhang, Y. Liu, Insulin promotes macrophage phenotype transition through PI3K/Akt and PPAR-gamma signaling during diabetic wound healing, J. Cell. Physiol. 234 (4) (2019) 4217–4231.

[57] J. Fu, M.G. Yu, Q. Li, K. Park, G.L. King, Insulin's actions on vascular tissues: physiological effects and pathophysiological contributions to vascular complications of diabetes, Mol. Metabol. (2021) 101236.

[58] J. Rankenberg, S. Rakete, B.D. Wagner, J.L. Patnaik, C. Henning, A. Lynch, M. A. Glomb, R.H. Nagaraj, Advanced glycation end products in human diabetic lens capsules, Exp. Eye Res. 210 (2021) 108704.

[59] J.B. Zhang, H. Li, L. Zhang, J.L. Wang, Observation of curative effect of recombinant human basic fibroblast growth factor combined with compound polymyxin B ointment and local application of insulin on wound healing of deep second-degree burn in diabetes mellitus: a randomized study, Eur. Rev. Med. Pharmacol. Sci. 23 (2019) 5987–5993.

[60] R.E. Mirza, M.M. Fang, W.J. Ennis, T.J. Koh, Blocking interleukin-1β induces a healing-associated wound macrophage phenotype and improves healing in type 2 diabetes, Diabetes 62 (2013) 2579–2587.

[61] F. Zhang, G. Banker, X. Liu, P.A. Suwanabol, J. Lengfeld, D. Yamanouchi, K. C. Kent, B. Liu, The novel function of advanced glycation end products in regulation of MMP-9 production, J. Surg. Res. 171 (2) (2011) 871–876.
[62] K. Herold, B. Moser, Y. Chen, S. Zeng, S.-F. Yan, R. Ramasamy, J. Emond, R. Clynes, A.M. Schmidt, Receptor for advanced glycation end products (RAGE) in a dash to the rescue: inflammatory signals gone awry in the primal response to stress, J. Leukoc. Biol. 82 (2) (2007) 204–212.
[63] S. Sudarsan, D.S. Franklin, M. Sakthivel, S. Guhanathan, Non-toxic, antibacterial, biodegradable hydrogels with pH-stimuli sensitivity: Investigation of swelling parameters, Carbohydr. Polym. 148 (5) (2016) 206–215.
[64] Sudarsan, M.S. Selvi, G. Chitra, M. Sakthivel, D.S. Franklin, S. Guhanathan, Non-toxic pH-sensitive silver nanocomposite hydrogels for potential wound healing applications, Polym. Plast. Technol. Mater. 60 (1) (2020) 84–104.
[65] G. Chitra, D.S. Franklin, S. Sudarsan, M. Sakthivel, S. Guhanathan, Non-cytotoxic silver and gold nanocomposite hydrogels with enhanced antibacterial and wound healing applications, Polym. Eng. Sci. 58 (12) (2018) 2133–2142.